This is to certify that the

thesis entitled

RHEOLOGICAL ANALYSIS OF STARCH-THICKENED, STRAINED
APRICOTS USING MIXER VISCOMETRY TECHNIQUES

presented by

Eugene William Ford

has been accepted towards fulfillment
of the requirements for

M.S. degree in Agricultural Engineering

James F. Steffe
Major professor

Date November 7, 1984

RHEOLOGICAL ANALYSIS OF STARCH-THICKENED, STRAINED APRICOTS USING MIXER VISCOMETRY TECHNIQUES

by

Eugene William Ford

A THESIS

Submitted to
Michigan State University
in partial fulfillment of the requirements
for the degree of

MASTER OF SCIENCE

Department of Agricultural Engineering

1984

ABSTRACT

RHEOLOGICAL ANALYSIS OF STARCH-THICKENED, STRAINED APRICOTS USING MIXER VISCOMETRY TECHNIQUES

by

Eugene William Ford

Three major problems were considered in performing a complete analysis on a starch-thickened, strained apricot puree: irreversible breakdown (thixotropy), loading shear breakdown and wall effects (slippage). Shear stress and shear rate were estimated from mixer viscometer data. A structural parameter, yield stress, flow behavior index and a consistency coefficient were defined to quantify the rate of breakdown and equilibrium structure of the product. The techniques developed in this study are useful in describing the time-dependent behavior of suspensions because the wall effect--due to slip--is minimized.

To:

Emily, thanks for putting up with me through all of this,
what an angel
William and Wanda Ford, my parents
Earnest and Jean Jones, my new parents
Roy, my brother
Tina, my sister
Lydia, my sister
thanks, all of you, for the support

ACKNOWLEDGMENTS

The author wishes to express his deepest gratitude to Dr. James F. Steffe, a teacher, advisor, and friend, for his moral and technical support.

The author is thankful to Dr. John B. Gerrish and Dr. Kris A. Berglund for serving on the guidance committee.

Thankful acknowledgments go to the Gerber Products Company which graciously supplied us with the funding, apricot puree and use of their pilot plant facilities necessary to complete this study.

A very special thanks goes to Marnie and Emily who made this all readable from my often unreadable manuscripts.

Special thanks goes to the faculty, staff and students of Michigan State University Departments of Agricultural Engineering and Food Science who made every step of the way enjoyable.

TABLE OF CONTENTS

Chapter Page

1. INTRODUCTION 1
    1.1. Theory of Starch Swelling and Use of Starch as a Thickening Agent 1
    1.2. Overview of Efforts 2
    1.3. Reasons for Study 3
    1.4. Objectives 3
2. LITERATURE REVIEW 6
    2.1. Properties of Starch and Fruit Purees . . . 6
        2.1.1. Starch Solutions 6
        2.1.2. Fruit Purees 7
        2.1.3. Starch-Thickened Fruit Purees . . . 8
    2.2. Thixotropy Characterization Methods 8
    2.3. Mixer Viscometry 14
    2.4. Wall Effects 15
3. THEORETICAL DEVELOPMENT 19
    3.1. Mixer Viscometry 19
    3.2. Modified Tiu and Boger Method of Breakdown Characterization 21
        3.2.1. Assumption of No Recovery and Basis of Model 21
        3.2.2. Use of Approximate Shear Rate and Approximate Shear Stress 24
    3.3. Krieger Analysis for Concentric Cylinder Viscometers 25
4. EXPERIMENTAL EQUIPMENT 27
5. PREPARATION OF THE STARCH-THICKENED, STRAINED APRICOTS 30

6. DATA COLLECTION AND ANALYSIS 33
6.1. Yield Stress Data Collection and Analysis . 33
6.1.1. Yield Stress at Initial Point of Breakdown (Time Zero) 33
6.1.2. Yield Stress at Equilibrium 34
6.2. Recovery Data Collection and Analysis . . . 36
6.3. Paddle Mixer Constant (k') Data Collection and Anaysis 38
6.4. Thixotropic Breakdown Data Collection and Analysis 39
6.5. Wall Effect Data Collection and Analysis at Equilibrium 41
6.6. Paddle Mixer Rheological Parameters Estimation 44
7. RESULTS AND DISCUSSION 45
7.1. Discussion of 45
7.1.1. Results of the Recovery Test 45
7.1.2. Results of the Breakdown Analysis . 45
7.1.3. Results of the Wall Effect Analysis 59
7.1.4. Results of the Paddle Mixer Test . . 63
7.1.5. Relationship Between Phenomenological Relationship and Equilibrium Rheogram 66
8. CONCLUSIONS 68
9. SUGGESTIONS FOR FURTHER STUDY 69
10. REFERENCES 70
11. APPENDICES 73
A. ANALYSIS OF STABILITIY OF STARCH
B. FLOW CHART OF ANALYSIS
C. OUTLINE OF DATA COLLECTION

LIST OF TABLES

Table Page

1. Models used to characterize thixotropy 9

2. Dimensions of the MV sensors and the MV paddle mixer 28

3. List of ingredients per 1000kg of finished product 31

4. Outline of statistics model used to check for wall effects 43

5. Data used to evaluate the mixer constant (k') for the MV paddle mixer 46

6. Experimental values of a_1 and $1/(\eta_{ao}-\eta_e)$ data obtained using the modified Tiu and Boger method 54

7. Torque at time zero and structural parameter data obtained using the modified Tiu and Boger method 55

8. Series of data and calculations used to determine yield stress at time zero 56

9. The β constants determined using the statistical model 60

10. Rheological data for Karo light corn syrup . . 61

11. Rheological parameters of starch-thickened, strained apricots obtained using various MV sensors and the MV paddle mixer 62

LIST OF FIGURES

Figure Page

1. Rheological classification of fluids 5

2. Paddle mixer schematic 35

3. Yield stress determination using stress to initiate flow 37

4. Plot used to evaluate the mixer viscometer constant (k') for the MV paddle mixer 47

5. Recovery after a) 10 minutes b) 60 minutes . 48

6. $1/(\eta_a - \eta_e)$ versus time at various shear rates . 50

7. a_1 versus shear rate 52

8. Rheogram obtained at time zero from modified Tiu and Boger analysis using the MV paddle mixer 53

9. Rheograms obtained using various MV sensors and the paddle mixer 64

10. Apparent viscosity versus shear rate obtained using various MV sensors and the MV paddle mixer 65

11. Apparent viscosity versus shear rate obtained from phenomenological relationship at equilibrium and equilibrium rheogram 67

NOMENCLATURE

A = constant, which depends on mixer system geometry, defined by Equation 12

a_1 = constant in Tiu and Boger's method defined by Equation 18

d = diameter of paddle mixer (m)

h = equivalent height of bob or sensor (m)

H_o = the null hypothesis

I_1, I_2 = dummy variables used in t-test for three linear equations

K = consistency coefficient ($Pa \cdot s^n$)

k' = paddle mixer constant needed for K approximation and shear rate approximation defined by Equation 13

K_o = initial consistency coefficient defined by Equation 15 ($Pa \cdot s^n$)

k_1 = rate constant, which is a function of shear rate, defined by Equation 16

M = torque ($N \cdot m$)

M_o = initial torque defined by Equation 31 ($N \cdot m$)

M_o' = torque to initiate flow ($N \cdot m$)

n = flow behavior index, dimensionless

n_o = initial flow behavior index defined by Equation 15, dimensionless

p = power ($J \cdot s^{-1}$)

Po = power number for mixing vessels defined by Equation 10, dimensionless

R_b = radius of bob or sensor (m)

R_c = radius of cup (m)

Re = Reynolds number, dimensionless

S = ratio of cup to bob radius defined by Equations 2, 3 and 4, dimensionless

s = Krieger's analysis variable defined by Equation 24

s' = Krieger's analysis variable defined by Equation 24

t = Student's t-distribution

v = slip velocity ($m \cdot s^{-1}$)

X_3 = ln (shear rate)

$\beta_o, \beta_1, \beta_2, \beta_3, \beta_4, \beta_5$ = constants in the t-tests for three linear equations defined in Equation 32

β' = effective slip coefficient

$\dot{\gamma}$ = shear rate (s^{-1})

$\dot{\gamma}_a$ = apparent shear rate (s^{-1})

η = fluid viscosity (assumes Newtonian fluid), ($Pa \cdot s$)

η_a = apparent viscosity ($Pa \cdot s$)

η_e = apparent viscosity at equilibrium ($Pa \cdot s$)

η_{ao} = initial apparent viscosity ($Pa \cdot s$)

λ = structural parameter defined by Equation 17

λ_e = structural parameter at equilibrium

ρ = density ($kg \cdot m^{-3}$)

τ_a = apparent shear stress (Pa)

τ_b = shear stress at bob (Pa)

τ_e = apparent shear stress at equilibrium (Pa)

τ_y = yield stess (Pa)

τ_{yo} = initial yield stress defined by Equation 15 (Pa)

Ω = angular velocity (s^{-1})

INTRODUCTION

1.1. Theory of Starch Swelling and Use of Starch as a Thickening Agent

Starch is a polysaccharide consisting of amylose (linear fraction) and amylopectin (branched fraction). It occurs naturally as discrete bundles or granules. When starch is mixed with water and the solution is heated to 60-75^{o}C, gelatinization occurs. During gelatinization, starch granules imbibe water until they break apart. Partial gelatinization leaves the starch in a very swollen state since the structure is only partially broken down. Gelatinization is caused by the hydrophilic groups in the starch molecule taking up moisture in proportion to the relative humidity of the atmosphere. An increase in temperature furnishes the energy required to break some of the intermolecular hydrogen bonds present in a starch system. This allows for paths of water entry and more pockets for water storage. Swelling occurs due to an increased amount of water being held in the starch structure. This swelling, in turn, thickens the water-starch solution because of the increased granule size, and thus increases the viscosity (Fennema, 1976).

Partially gelatinized starch solutions are often used to thicken products which are thinner than the consumer prefers, e.g. apricot baby food manufactured by the Gerber Products Company and used in this study. It is the study of these products on which this paper will focus.

1.2. Overview of Efforts

This study includes four general areas of experimentation. First, apricot puree samples were mechanically degraded with a mixer driven at a constant angular velocity until consistencies reached equilibrium. After a 10 or 60 minutes recovery period, a second mechanical degradation curve was obtained. The degree of recovery of the initial structure was determined by comparing the second degradation curve with the first for each sample. The extent of recovery dictated the nature of the apricot puree breakdown, i.e. reversible, partially reversible or irreversible.

Following the recovery analysis, the breakdown and build-up (if applicable) curves were characterized using a model developed by Tiu and Boger (1974). The model was modified to account for the completely irreversible breakdown which apricot puree seems to undergo. (See Figure 1 for rheological classification of fluids.)

Next, the problem of wall effects, which can occur in suspensions, was investigated using samples which had been mechanically degraded to their equilibrium structures. Wall effects can be caused by localized separation (thinning) at the sensor, or by an even settling of solids within the entire sample. Wall effects may be a problem particularly with narrow gap viscometers, such as the one used in this study.

Finally, the possibility of using a mixer viscometer instead of a narrow gap concentric cylinder viscometer was investigated. The value of the mixer is that it would keep product solids suspended, thereby minimizing product thinning near the sensor. In addition, a sample type mixer would tend to minimize sample degradation while loading the cup into the viscometer.

1.3. Reasons for Study

To date, there has not been a complete characterization of a starch-thickened fruit puree presented in the literature. A complete anlysis includes characterization of recovery, breakdown and build-up (if applicable) curves, wall effects and the equilibrium rheogram. Secondly, it has not yet been determined if wall effects are a problem when using concentric cylinder viscometers, and if wall effects are present, how to minimize them when testing food suspensions. Finally, the results of this study will be invaluable in formulating rheologically based quality control tests for starch-thickened products.

1.4. Objectives

The major objective of this study was to conduct a complete rheological analysis of starch-thickened apricot puree. A secondary objective was to determine whether or not a paddle mixer viscometer could be used to overcome problems which concentric cylinder viscometers have with suspended solids. These problems included loading shear breakdown in the mechanical degradation tests and separation of sample near the bob (wall effects) in the equilibrium tests.

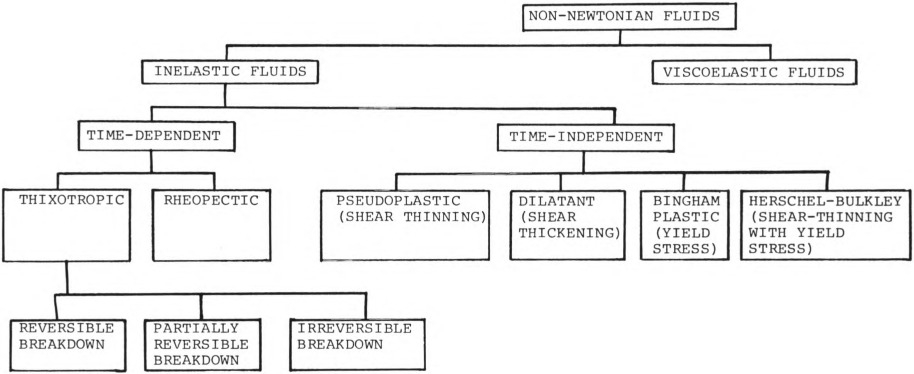

Figure 1. Rheological classification of fluids.

LITERATURE REVIEW

2.1. Properties of Starch and Fruit Purees

2.1.1. Starch Solutions

Pure starch solutions have been shown to have partially reversible breakdown at a constant shear rate by Evans and Haisman (1979), Howling (1980), and Lang and Rha (1981). The extent of swelling (percent gelatinization) can be correlated with viscosity behavior (Schoch, 1969). Specifically, a large amount of swelling results in fragile granules which are readily fragmented (from the breaking of intermolecular hydrogen bonds) upon stirring, thereby resulting in a substantial thinning of the starch solution. This fact contributes to the irreversible component of the partially reversible breakdown exhibited by starch solutions.

It is possible that the corresponding reversible component is, in part, due to slip, i.e. the formation of a thinner solution layer near the bob (sensor) during shearing. Specifically, the redistribution of the sample to homogeneity (reversal of slip) during the recovery period could result in a torque pattern which erroneously suggests reversibility. Traditional theories used to quantify thixotropy (Cheng and Evans, 1965; Hahn et al., 1959 and Harris, 1972) ignore the possible presence of slip in the sample. Van Wazer et al. (1963), Figoni and Shoemaker (1981) and Rao (1975) suggested that there may be slip in the starch suspensions when using contemporary coaxial and cone-and-plate viscometers, but no remedy was offered. Evans and Haisman (1979) measured sedimentation rates but never studied the possibility of sedimentation causing a thinner liquid to be near the bob, thus resulting in erroneous data.

2.1.2. Fruit Purees

Apricot puree was studied by Harper (1960) and Watson (1968). These authors reported the material to be shear-thinning, at various solids contents and over a wide range of ripeness. Other data can be found for apple sauce (Charm, 1962; Haugen and Tung, 1976; Saravacos and Moyer, 1967; Saravacos, 1968; Steffe et al., 1984) tropical fruit purees--banana, guava, mango, papaya--(Rao, et al., 1974), peach puree (Harper, 1960; Saravacos and Moyer, 1967) and plum puree (Saravacos and Moyer, 1967). Data from the above and other related articles have been summarized in a recent paper by Steffe et al. (1983). Also, it should be noted that all of the fruit products mentioned above were modelled as power-law fluids, meaning no significant yield stress was observed.

Duran and Costell (1982) observed thixotropy, i.e. time-dependent flow, in four varieties of apricot puree. Canovas and Peleg (1983) observed similar behavior in commercial semi-liquid food products, such as apple sauce, banana puree and peach puree. Both of these studies used the Herschel-Bulkley model to describe equilibrium structure. (Some of the products tested by Canovas and Peleg were starch-thickened.)

2.1.3. Starch-Thickened Fruit Purees

To date, there has not been a complete analysis of starch-thickened fruit puree in the literature. Although Canovas and Peleg (1983) tested some starch-thickened products, they did not discuss the possibility of wall effects, i.e. product separation, causing time-dependent flow, nor did they quantify the breakdown curve.

2.2. Thixotropy Characterization Methods

As stated earlier, thixotropy has been observed in starch-thickened fruit products. Table 1 presents an outline of methods used to characterize this phenomenon.

The first two methods listed are based on a hysteresis loop, which is obtained in the following manner:

1. Angular velocity of the bob of a rotational viscometer is steadily increased from zero to a chosen maximum angular velocity in a specific time, t.
2. Angular velocity is then steadily decreased back to zero in the same time, t.

Steps 1 and 2 can be carried out with a speed programmer or with periodic changes in angular velocity by manual manipulation. The data can be plotted in two ways: a) shear stress can be plotted against time on an x-t plotter (then, since shear rate varies linearly with time,

Table 1. Models used to characterize thixotropy.

*Type of Experiment	Constants	Basis of Characterization	References
Hysteresis Loop	0	1. assumed complete recovery 2. assumed build-up and breakdown rate equal 3. no yield stress determination necessary 4. measurement of area under hysteresis loops used to determine the difference between samples, no absolute basis	Green and Weltman (1943) Heywood (1981)
Hysteresis Loop	2	1. assumed complete recovery 2. assumed build-up and breakdown rate equal 3. no yield stress determination necessary 4. divided breakdown into two components: a coefficient of breakdown with time and a coefficient of breakdown due to increasing shear rate	Green and Weltman (1943)
Equilibrium Flow Curve	5	1. assumed complete recovery 2. assumed build-up and breakdown rates different 3. yield stress determination necessary 4. Bingham plastic fluid assumed 5. a phenomenological relationship and rate equation were used 6. structural parameter used which is less than or equal to unity at all times 7. equilibrium curve and step change in shear rate tests required for complete analysis	Cheng and Evan (1965); Heywood (1981)
Step Change in shear rate	7	1. assumed complete recovery 2. assumed build-up and breakdown rate equal 3. no yield stress determination necessary 4. Herschel-Bulkley fluid assumed 5. a phenomenological relationship and rate equation were used	Kemblowski and Petera (1979)

Table 1. Models used to characterize thixotropy (cont.).

*Type of Experiment	Constants	Basis of Characterization	References
Step Change in shear rate (continued)		6. structural parameter used which is quite different from Cheng's, i.e. the value of the constant ranges from zero to infinity according to what structural level is present 7. step change in shear rate used to do the characterization 8. produces a 4 plot presentation of the breakdown and equilibrium curves, very elaborate	
Step Change in shear rate	9	1. same as above except 2. yield stress determination necessary 3. assumed build-up and breakdown rates different 4. even more elaborate than the previous method	Kemblowski and Petera (1980)
Breakdown Cruve Anaysis	5	1. assumed complete recovery 2. assumed build-up and breakdown rate equal 3. yield stress determination necessary 4. Herschel-Bulkley fluid assumed 5. an equation of state and rate equation were used 6. a structural parameter similar to Cheng's was used 7. all constants are determined using the breakdown curves at different angular velocities	Petrellis and Flummerfelt (1973) Tiu and Boger (1974)

*assumed only viscous nature, i.e. no elastic properties shear rate at any t can be determined), b) shear stress can be plotted against shear rate on an x-y plotter.

Hysteresis loops are presently used for quick qualitative analysis of a thixotropic material. By measuring the area under the hysteresis loop, the relative thixotropic behavior of a group of samples can be determined (Heywood, 1981). It should be noted that the surface area of the hysteresis loop depends on the previous history of the sample, the maximum shear rate and the acceleration. Too fast an acceleration may induce hysteresis in a non-thixotropic material, since kinetic energy on the deceleration side of the loop may decrease the torque needed to turn the bob.

Green and Weltman (1943) attempted to use loops quantitatively by relating the area of the hysteresis curve to the degree of thixotropy, using two coefficients: a coefficient of thixotropic breakdown with time and a coefficient of thixotropic breakdown due to increasing shear rate. Heywood (1981) stated that because Green and Weltman carried out their analysis on the first loop obtained, reproducibility was poor since the condition of the material prior to shear testing was critical. If an "equilibrium loop", obtained after repeated cyclings of the hysteresis loop until the loops superimposed, were used, reproducibility would be greatly improved. However, the equilibrium method can not be used with irreversible thixotropic materials, since the acceleration and deceleration sides of the loop coincide at equilibrium, making determination of the two coefficients impossible.

Cheng (1956) presented a method of obtaining quantitative information on thixotropic behavior above yield stress, using a Bingham Plastic model as the basis and adding a structural parameter, λ. Time-dependence was assumed to be due to changes in λ. A phenomenological relationship (Bingham Plastic model with λ) and a rate equation (change in λ with respect to time) were used to describe thixotropic behavior. Cheng used an equilibrium flow curve to determine the constants for the two equations. After breaking down the sample structure, torque readings were taken over a range of shear rates and the equilibrium flow curve was drawn, i.e. shear stress was plotted against shear rate. It should be noted that the final step in this method requires complete recovery making this method invalid for irreversible products.

Kemblowski and Petera (1979) presented a model for describing thixotropic behavior based on a structural parameter different from that presented by Cheng, which was introduced in a phenomenological manner without reference to its physical meaning. Two starting assumptions were made: a) A thixotropic fluid's equilibrium behavior can be described using the power-law model, b) Under isothermal conditions, the influence of all variables except shear rate may be described by one scalar value, the structural parameter. Like Cheng, Kemblowski and Petera developed a phenomenological relationship and a rate equation based on a structural parameter.

Experiments, designed to find the constants required in the phenomenological relationship and rate equation, of the "step-change in shear rate" type were used. (In step-change in shear rate tests, a sample is sheared at a particular shear rate to equilibrium, after which the shear rate is abruptly lowered. The build-up of sample structure is then monitored. Finally, the original shear rate is employed and sample structure breakdown is followed.) Using the build-up and breakdown curves, the appropriate constants were calculated and the thixotropic phenomenon could be completely described mathematically. Kemblowski and Petera's original method (1979) is very complex, although the rate of structure build-up is assumed to be equal to the rate of structure breakdown. In a follow-up paper, Kemblowski and Petera (1980) outlined a slightly more involved method of description, which included yield stress determination and techniques for independently determining build-up and breakdown rates, instead of assuming them equal.

Tiu and Boger (1974), basing their work on the model by Petrellis and Flummerfelt (1973), started with the Herschel-Bulkley equation. To account for time-dependent effects, a structural parameter, λ , similar to Cheng's was added. As in the previously mentioned methods, a phenomenological relationship and a rate equation based on the structural parameter were used to describe thixotropy. The balance of Tiu and Boger's paper was devoted to developing experiments and deriving equations for the determination of the necessary constants. Specifically, a series of breakdown curves run at various shear rates were used. (A breakdown curve is the change in torque with time at consant shear rate.) It is important to note that Tiu and Boger's model was only applied in the non-destructive range of shear rate, i.e. they assumed total recovery.

Certain other methods are worth noting since they are based on assumptions different from those underlying the previously mentioned methods. Harris (1967) used a relaxation spectrum and an associated memory function to describe reversible thixotropy. A method which uses the Bird-Leider equation, which mathematically takes into account the viscous and elastic properties of the samples, was presented by Dickie and Kokini (1982, 1983). Most of the other methods reviewed by the author were based on similar or the same assumptions underlying the methods previously listed in this study or were empirical in nature and apply only to the product used in the study.

2.3. Mixer Viscometry

Metzner and Otto (1957) presented a method of approximating power-law parameters for non-Newtonian fluids using apparent viscosity calculated from data obtained with a mixing vessel. Rieger and Novak (1973) outlined a method to determine whether or not shear rate is a linear function of angular velocity for a given paddle mixer and, if linear, how to determine the paddle mixer's proportionality constant.

Rao (1975) presented a method, based on the aforementioned techniques, of approximating power-law parameters for food suspensions, such as starch-thickened products. These products could not be characterized with narrow gap viscometers due to the size and possible separation and settling of particles, i.e. formation of a dilute phase near the bob. The Rao method (1975) is an approximation since only an average shear rate can be determined due to varying shear rate from point to point on the paddle mixer.

2.4. Wall Effects

According to Whorlow (1980), apparent slippage due to material properties changing near walls can be detected by using two or more sensors (bobs) with sensor radii different, sensor heights equal and a similar cup radius. If the same shear stress/shear rate flow curve is generated by all the sensors, no wall effects are present; but if different flow curves are drawn for each sensor, a wall effect is present. In this study, the above consideration was used in testing for the presence of wall effects.

Wall effects in concentric cylinder viscometers can be characterized using slip velocities (Oldroyd, 1956) or by using an effective slip coefficient (Mooney, 1931). The method by Oldroyd (1956, not seen, cited by Whorlow, 1980) assumes that the slip velocity, v, depends only on the shear stress at the wall. The total angular velocity, Ω, of the bob with respect to the stationary cup is given by:

$$\Omega = \frac{1}{2}\int_{\tau_c}^{\tau_b} \frac{\dot{\gamma}(\tau)}{\tau}\, d\tau + \frac{v(\tau_b)}{R_b} + \frac{v(\tau_c)}{R_c} \tag{1}$$

where,

R_b = radius of bob (m)
R_c = radius of cup (m)
v = slip velocity ($m \cdot s^{-1}$)
τ = shear stress ($N \cdot m^{-2}$)
$\dot{\gamma}$ = shear rate (s^{-1})

If R_b is varied, and R_c and τ_c are kept constant,

$$\Omega \to 0 \quad \text{as} \quad R_b \to R_c$$

but due to slip,

$$\Omega \to \frac{2v(\tau_c)}{R_c} \quad \text{as} \quad R_b \to R_c$$

Mooney's method (1931) as presented in Skelland (1967), defines S as the ratio of cup to bob radius. Then,

$$S_a = \frac{R_2}{R_1} \tag{2}$$

$$S_b = \frac{R_3}{R_2} \tag{3}$$

$$S_c = \frac{R_3}{R_1} \tag{4}$$

where,

$$R_1 < R_2 < R_3$$

The angular velocities required to yield the same torque, M, with S_a, S_b and S_c are then measured as Ω_a, Ω_b and Ω_c, respectively. The following equation is used to calculate the effective slip coefficient, β', at the surface, $2\pi R_2 h$:

$$\beta' = \frac{2\pi^2 R_2^{\ 2}}{M} \quad (\Omega_a + \Omega_b - \Omega_c) \tag{5}$$

By repeating this procedure at other values of M, the relationship between β' and τ_2 can be determined by linear regression, after calculating β' with Equation 5 and τ_2 using Equation 6 below:

$$\tau_b = \frac{M}{2\pi (R_b)^2 h} \tag{6}$$

where,

h = equivalent height of bob (m)

τ_b = shear stress at bob ($N \cdot m^{-2}$)

To determine effective slip corrections, effective slip velocities at the bob and cup are calculated using:

$$v_b = \beta_b \ \tau_b \tag{7}$$

$$v_c = \beta_c \ \tau_c \tag{8}$$

where,

v_b = slip velocity at bob ($m \cdot s^{-1}$)

v_c = slip velocity at cup ($m \cdot s^{-1}$)

β_b = effective slip coefficient at bob

β_c = effective slip coefficient at cup

τ_b = shear stress at bob ($N \cdot m^{-2}$)
τ_c = shear stress at cup ($N \cdot m^{-2}$)

and τ_b and τ_c are calculated using Equations 6 and 9, respectively.

$$\tau_c = \frac{M}{2\pi (R_c)^2 h} \tag{9}$$

The effective slip coefficients, β_b and β_c, are determined using τ_b and τ_c, respectively, on the β' versus τ_2 curve.

The true shear rate corresponding to τ_b is estimated by multiplying the calculated shear rate (section 3.3) by the ratio of the actual velocity difference (from cup to bob) to the velocity difference without slip.

The two methods outlined in this section were not used to characterize wall effects in this study since the viscometer used did not conform to the geometry required by Mooney's method, nor could it yield the angular velocities required to yield the same torque for all three sensors required by both Oldroyd's and Mooney's methods. First, one of the geometry requirements of Mooney's method is that one of the two cup radii must equal one of the two bob radii. The viscometer used in the present study was equipped with one cup and three bobs. Second, a constant angular velocity viscometer was used, while both methods required a constant torque viscometer.

THEORETICAL DEVELOPMENT

3.1. Mixer Viscometry

The power consumption in a mixing vessel for Newtonian fluids can be expressed in terms of a power number (Metzner and Otto, 1957, cited by Rao, 1975),

$$Po = p/(d^5 \Omega^3 \rho) \tag{10}$$

and a mixing Reynolds number,

$$Re = d^5 \Omega \rho / \eta \tag{11}$$

as

$$Po = A/Re \tag{12}$$

where,

A = constant depending on system geometry (dimensionless)

d = impellor diameter (m)

p = power (Torque x Angular velocity) ($N{\cdot}m{\cdot}s^{-1}$)

Po = power number (dimensionless)

η = fluid viscosity (Pa·s)

ρ = density ($kg{\cdot}m^{-3}$)

Ω = angular velocity (s^{-1})

Metzner and Otto (1957) suggested that Equation 12 could be used for non-Newtonian fluids if an apparent viscosity were used. This apparent viscosity was calculated at an average shear rate, which was determined by the following equation:

$$\dot{\gamma}_a = k' \ \Omega \tag{13}$$

where,

k' = paddle mixer constant

$\dot{\gamma}_a$ = apparent (average) shear rate (s^{-1})

This relationship was shown to be valid for a particular impellor if a plot of log $(p/(K\Omega^{n+1}d^3))$ versus (1-n) was a straight line. The slope of the straight line was determined as -log k' (Rieger and Novak, 1973). If the plot were nonlinear, Equation 13 would be invalid since k' would not exist. The rotation Reynolds number, Re = $\Omega^{n-2} d^2 p/k$, must be less than 10 for the flow conditions to be laminar as assumed.

For any type of sensor, including the paddle mixer, the flow behavior index, n, is equal to the slope of the log (torque in N·m) versus log (angular velocity in s^{-1}). The consistency coefficient, K, is determined using the following relationship between test sample, x, and a standard fluid, s, having known rheological properties (Rao, 1975):

$$K_x = \frac{M_x}{M_s} \cdot \frac{(\Omega k')^{n_s}}{(\Omega k')^{n_x}} \cdot K_s \tag{14}$$

where,

K_s = consistency coefficient for standard fluid (Pa·s^n)

K_x = consistency coefficient for test sample (Pa·s^n)

M_s = torque at chosen angular velocity for standard fluid (N·m)

M_x = torque at chosen angular velocity for test sample (N·m)

n_s = flow behavior index for standard fluid (dimensionless)

n_x = flow behavior index for test sample (dimensionless)

Equation 14 assumes power law fluid (no yield stress).

3.2. Modified Tiu and Boger Method of Breakdown Characterization

3.2.1. Assumption of No Recovery and Basis of Model

Most of the literature defines thixotropy as a completely reversible process (Hahn et al., 1959; Van Wazer et al., 1963; Cheng and Evans, 1965 and Sheth, 1976) so researchers who have developed methods to characterize thixotropy have followed this general consensus and have assumed complete recovery. (See Literature Review for an outline of the most pertinent methods.) Herein lies the major problem in mathematically describing breakdown of starch-thickened apricot puree. While the available models assume complete recovery (usually at the same rate as breakdown), the apricot puree exhibits only partial recovery at best and usually no recovery at all.

Although all known methods assume complete recovery, two do not depend on recovery in their derivation. The first of these two methods, the hysteresis loop area test, was not used in this study because the test only gives a relative indication of thixotropic behavior of a group of samples (Heywood, 1981). The second method, breakdown curve analysis (Petrellis and Flummerfelt, 1973, as referenced by Tiu and Boger, 1974), yields absolute data and is therefore more repeatable than the hysteresis loop area test. For this reason, breakdown curve analysis, with three modifications, was the method of choice for this study. The initial modification was the assumption of complete irreversibility, i.e. no recovery, for the apricot puree.

Changes were also made in the methods of calculating shear stress and shear rate.

Tiu and Boger (1974) characterized product breakdown curves with two basic equations. The phenomenological relationship

$$\tau = \lambda\ [\tau_{y_o} + K_o\ \dot{\gamma}^{n_o}] \qquad (15)$$

where,

K_o = consistency coefficient at time zero (Pa·s^n)

n_o = flow behavior index at time zero (dimensionless)

λ = structural parameter (equal to unity at time zero and to an equilibrium value, λ_e, at equilibrium) (dimensionless)

τ_{y_o} = yield stress at time zero (N·m)

is basically the Herschel-Bulkley equation with structural parameter, λ, added. The rate equation is

$$\frac{d\lambda}{dt} = -\ k_1\ (\lambda - \lambda_e)^2 \qquad (16)$$

where,

k_1 = rate constant which is a function of shear rate

λ_e = equilibrium structural parameter (dimensionless)

$\frac{d\lambda}{dt}$ = change in structural parameter with respect to time

Since the structural parameter is equal to unity at zero shear time, Tiu and Boger defined the phenomenological relationship at time zero and calculated τ_{y_o}, K_o and n_o at that point. To determine the other two constants, k_1 and λ_e, the apparent viscosity was used. By equating shear stress in the phenomenological relationship with shear stress in the apparent viscosity equation, the structural parameter is defined as

$$\lambda = \frac{\eta_a \dot{\gamma}}{\tau_{y_o} + K_o \dot{\gamma}^{n_o}} \tag{17}$$

where,

η_a = apparent viscosity ($\eta_a = \frac{\tau}{\dot{\gamma}}$) (Pa·s)

By differentiating Equation 17 with respect to time and substituting for $\frac{d\lambda}{d\tau}$ in the rate equation and substituting Equation 17 for λ where appropriate, the change in apparent viscosity with respect to time is found to be

$$\frac{d\eta_a}{d\tau} = -a_1 (\eta_a - \eta_e)^2 \tag{18}$$

where,

η_e = apparent viscosity at equilibrium (Pa·s)

and

$$a_1(\dot{\gamma}) = \frac{k_1 \dot{\gamma}}{\tau_{y_o} + K_o \dot{\gamma}^{n_o}} \tag{19}$$

Integrating Equation 18 at constant shear rate from $\eta_a = \eta_{ao}$ at $t = 0$ to $\eta_o = \eta_a$ at $t = t$ yields

$$\frac{1}{\eta_a - \eta_e} = \frac{1}{\eta_{ao} - \eta_e} + a_1 t \tag{20}$$

where,

η_{ao} = apparent viscosity at time zero (Pa·s)

For a given shear rate, a plot of $1/(\eta_a - \eta_e)$ versus t yields a straight line whose slope is a_1. Repeating this procedure at different shear rates gives the relationship between a_1 and shear rate and therefore, by substituting a_1 $(\dot{\gamma})$ into Equation 19, the relationship between k_1 and shear rate.

By cross-plotting the shear stresses at time zero from breakdown curves at various shear rates against the corresponding shear rates, the parameters K_o, n_o and τ_{y_o} can be determined by linear regression using the Herschel-Bulkley model.

Finally, the equilibrium structural parameter can be calculated using

$$\lambda_e = \frac{\eta_e \dot{\gamma}}{\tau_{y_o} + K_o \dot{\gamma}^{n_o}} \tag{21}$$

Then, k_1, K_o, n_o, τ_y and λ_e can be substitutued into the phenomenological relationship and the rate equation to complete the analysis.

3.2.2. Use of Approximate Shear Rate and Approximate Shear Stress

Since a paddle mixer was used to minimize loading shear breakdown and possible wall effects, an approximate shear rate calculated using Equation 13 was used in the Tiu and Boger model. Shear stress, like shear rate, can only be approximated when using a paddle mixer. Shear stress was estimated using the idea that torque is directly proportional to stress (Rao, 1975):

$$\frac{M_x}{M_s} = \frac{\tau_x}{\tau_s} \tag{22}$$

meaning that,

$$\tau_{a_x} = \frac{\tau_s}{M_s} M_x \tag{23}$$

where,

τ_{a_x} = approximate shear stress for test sample ($N\cdot m^{-2}$)

τ_s = shear stress for standard solution ($N\cdot m^{-2}$)

τ_x = shear stress for test sample ($N\cdot m^{-2}$)

Using a standard fluid of known properties (a power-law fluid whose properties have been determined using a concentric cylinder viscometer), the value of shear stress, τ_s, can be determined from the power-law equation at a given shear rate calculated using Equation 13. M_s is read by a mixer viscometer running at the same shear rate at which τ_s is calculated. A series of shear rates could be used to verify that τ_s/M_s is constant for all shear rates. However, this is not necessary since shear stress is always a linear function of torque.

3.3. Krieger Analysis for Concentric Cylinder Viscometers

Krieger (1968) suggested the following method for calculating shear rates at the bob of a concentric cylinder viscometer:

$$\dot{\gamma} = \frac{2\Omega}{s}\left[\frac{R_c^{2/s}}{R_c^{2/s}-R_b^{2/s}}\right]\left[1 + s^2 s' \, f\left(\frac{2}{s}\ln\frac{R_c}{R_b}\right)\right] \qquad (24)$$

where,

$$\frac{1}{s} = \frac{d(\ln \Omega)}{d(\ln \tau_b)}$$

$$s' = \frac{d\ (1/s)}{d(\ln \tau_b)}$$

$$s^2 = s\cdot s$$

$$f(t) = \frac{t(e^t(t-2)+t+2)}{2(e^t-1)^2}$$

In the preliminary studies of this project, the second derivative term, s', in Krieger's shear rate approximation (Equation 24) was found to be insignificant, and thus Equation 24 reduced to

$$\dot{\gamma} = \frac{2\Omega}{s}\left[\frac{R_c^{2/s}}{R_c^{2/s} - R_b^{2/s}}\right] \qquad (25)$$

For concentric cylinder viscometers, shear stress is calculated using Equation 6.

EXPERIMENTAL EQUIPMENT

A Haake RV-12 viscometer (measuring head M500) with MVI, MVII and MVIII sensors (bobs) and MV paddle mixer sensor was used to generate rheological data. The system had a concentric cylinder geometry with the MV series sensors and was a mixing unit with the paddle mixer sensor. Table 2 shows the dimensions of these sensors.

Table 2. Dimensions of the MV sensors and the MV paddle mixer.

Sensor	R_b(m)	Equivalent height (h in meters)
[+]MVI	0.02004	0.06032
[+]MVII[*]	0.01840	0.05859
[+]MVIII	0.01520	0.06210
	Diameter (d in meters)	Height (m)
[+]paddle mixer	0.04143	0.02692

[+] The radius of the cup (R_c) is 0.021 m in all cases.

[*] The MVII sensor was made at Michigan State University from an MVI sensor. The length dimension is slightly smaller than a true MVII sensor.

A Haake speed programmer and a Haake F3-C temperature-controlled water circulator were used to set angular velocity and to maintain isothermal conditions, respectively. A Hewlett-Packard 85 computer and a Hewlett-Packard 3497 Data Acquisition/Control Unit were interfaced to the system to facilitate data collection. All tests were run with samples maintained at 25C ($\pm$ .01^{o}C).

PREPARATION OF THE STARCH-THICKENED, STRAINED APRICOTS

A batch of strained apricots thickened with tapioca starch (Table 3) was made in the pilot plant of the Gerber Products Company located in Fremont, Michigan. The ingredients were mixed, and the product was cooked by steam infusion, which caused starch gelatinization and subsequent thickening. After cooking, the product was sealed in 4.5 oz. (128g) jars and was cooled to room temperature in preparation for storage.

The tapioca starch investigated was on acetylated di-starch phosphate. The starch is a cross-linked product made by reacting the starch with sodium trimetaphosphate: the cross-bond is achieved through a phosphate ester linkage. The starch is also stabilized, against gel formation, by acetylation.

Table 3. List of ingredients per 1000kg of finished product.

Ingredients	kg/1000kg of finished product
*Apricot Concentrate 32 Brix	181.00
Sugar (white, granulated)	70.00
Tapioca Starch	44.00
Vitamin C	.28
Citric Acid	to pH 4.0
**Water	704.72

*Fruit is strained through a .020 in. (.051 cm) screen.

**Small quantity of water is added by steam infusion.

The tapioca starch has approximately 1.7% acetyl groups, as determined by the following analysis:

1. 5.0g of predried, modified starch was weighted and placed in a 250ml Erlenmeyer flask. (A sample of unmodified starch was used as a blank.)
2. 50ml distilled water was added and the mixture was swirled to suspend the starch.
3. 10 drops of phenolphthalein indicator was added.
4. .1N Sodium Hydroxide was used to titrate to a pink endpoint.
5. 25.0ml of 0.45N Sodium Hydroxide was added, taking care not to wet the neck of the flask.
6. The flask was then sealed tightly with a rubber stopper and was shaken vigorously for 30 minutes on a mechanical shaker.
7. The stopper was carefully removed and washed down together with the walls of the flask, with a fine stream of distilled water.
8. 0.500N HCl was used to titrate to the disappearance of the phenolphthalein color.
9. %Acetyl Groups = (ml needed for blank - ml needed for sample)

   X normality of the HCl X 0.043 X 100 /
   Sample Weight in Grams (dry basis)

Stabilizing the starch by acetylation allowed testing of the samples over a several month period without significant changes occuring in sample structure. (Appendix 1 presents starch stability as a function of elapsed time after processing.)

DATA COLLECTION AND ANALYSIS

6.1. Yield Stress Data Collection and Analysis

Both methods of yield stress determination mentioned in this section are only approximations. Special equipment, which was unavailable, is required for more accurate determination of yield stress (DeKee, et al. 1980 and Vocadlo and Charles, 1971). Yet, even the methods using special equipment can only approximate yield stress. Thus, due to the approximation needed to determine yield stress, great error in the low range of yield stress is possible. (Apricot puree has a very small or no yield stress.)

6.1.1. Yield Stress at Initial Point of Breakdown (Time Zero)

The method used in this study was the extrapolation of shear stress/shear rate data (20-120 rpm) to the shear stress (y) intercept, i.e. the yield stress. Data at time zero were gathered by using torque-versus-time curves from breakdown (thixotropic) analysis at different angular velocities. The initial torque reading of each breakdown curve was defined as the torque at time zero at that angular velocity. Then, a plot of torque at time zero versus shear rate was made and extrapolated to determine yield stress, which was the y-intercept.

In this study, the paddle mixer was used to minimize loading shear degradation. With a narrow gap viscometer, significant degradation of the sample can be caused when the sample is forced through the narrow gap between the inside and outside cylinders during loading. With the paddle mixer, loading degradation is kept to a minimum due to the paddle geometry (Figure 2).

Since the paddle mixer was used, approximate shear rates and aproximate initial shear stresses (the latter calculated from torque at time zero data) were calculated using Equations 13 and 23, respectively. The linear regression model, $y = ax^b + c$ (transformed as $\ln (y-c) = \ln a + b\ln x$ before use), was used to find the shear stress intercept that gave the best fit, i.e. the curve with lowest standard deviation. The variable, c, was defined as the yield stress at time zero, τ_{y_o}.

6.1.2. Yield Stress at Equilibrium

Two ways of yield stress determination were used at equilibrium: 1) extrapolation of shear stress/shear rate data (10-120 rpm) and 2) "torque-to-initiate-flow". The extrapolation procedure used at equilibrium was identical to that used in section 6.1.1., but data were collected in a slightly different manner. Specifically, since the product was at equilibrium, there was no concern over degradation, so the MVI sensor was used. (Equilibrium was reached by shearing the sample for 10 minutes at 60 rpm, using the paddle mixer.) Then, Equations 25 and 6 were used to calculate shear rate and shear stress, respectively.

The torque-to-initiate-flow test was performed at equilibrium, but not at the initital point of breakdown,

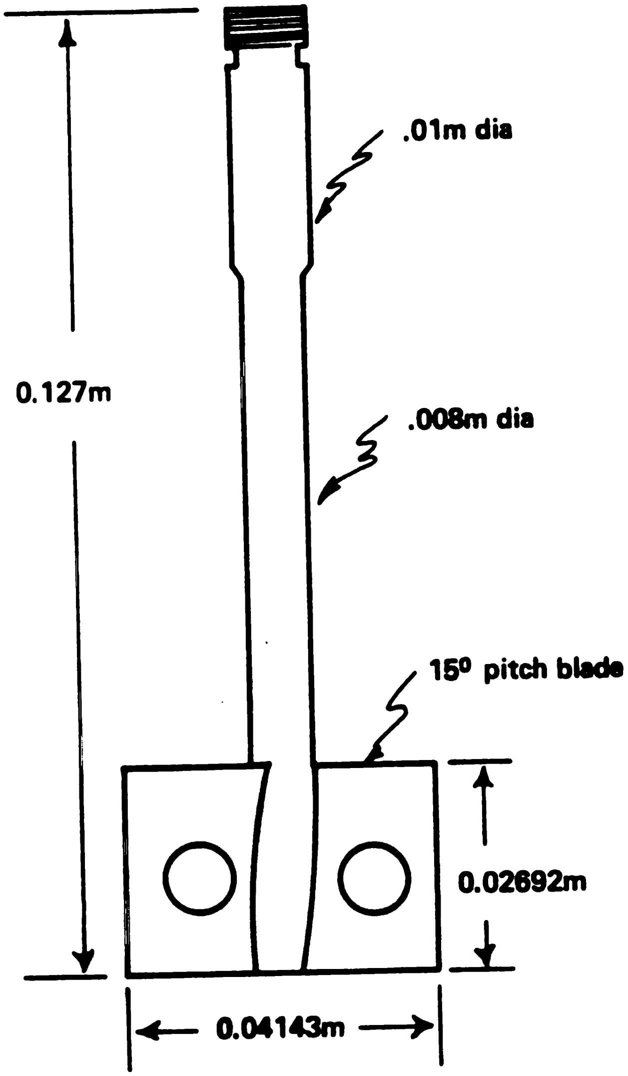

Figure 2. MV paddle sensor.

because at breakdown the yield point, B, would be lowered due to degradation of the sample while the torque was approaching the yield point (Figure 3). After the sample was degraded for 10 minutes at 60rpm using the paddle mixer, the paddle was exchanged for the MVI sensor. The angular velocity was set at the lowest possible speed which would allow yield stress to be reached before the completion of the data collection cycle (less than three seconds). A torque versus time plot was drawn by the HP 85, and the maximum, B, was defined as the torque at yield, which is related to yield stress by Equation 6 (Figure 3).

6.2. Recovery Data Collection and Analysis

To determine the extent of reversibility, the sample was first sheared for 10 minutes at 60 rpm with the paddle mixer, which was used instead of the MVI concentric cylinder to minimize loading shear and to maintain the sample suspension. After the 10 minute breakdown period, one set of samples was allowed to recover for 10 minutes while a second set was allowed to recover for 60 minutes. (The viscometer was turned off during the recovery period.) 10 and 60 minute recovery periods were chosen. With both sample sets, a second 10 minutes breakdown was performed following the recovery period. If the sample exhibited complete recovery, i.e. complete reversibility, presumeably at the same rate as initial breakdown, then the sample would build-up to the original structure by the end of the 10 minute recovery period. Thus, if superimposed, the second

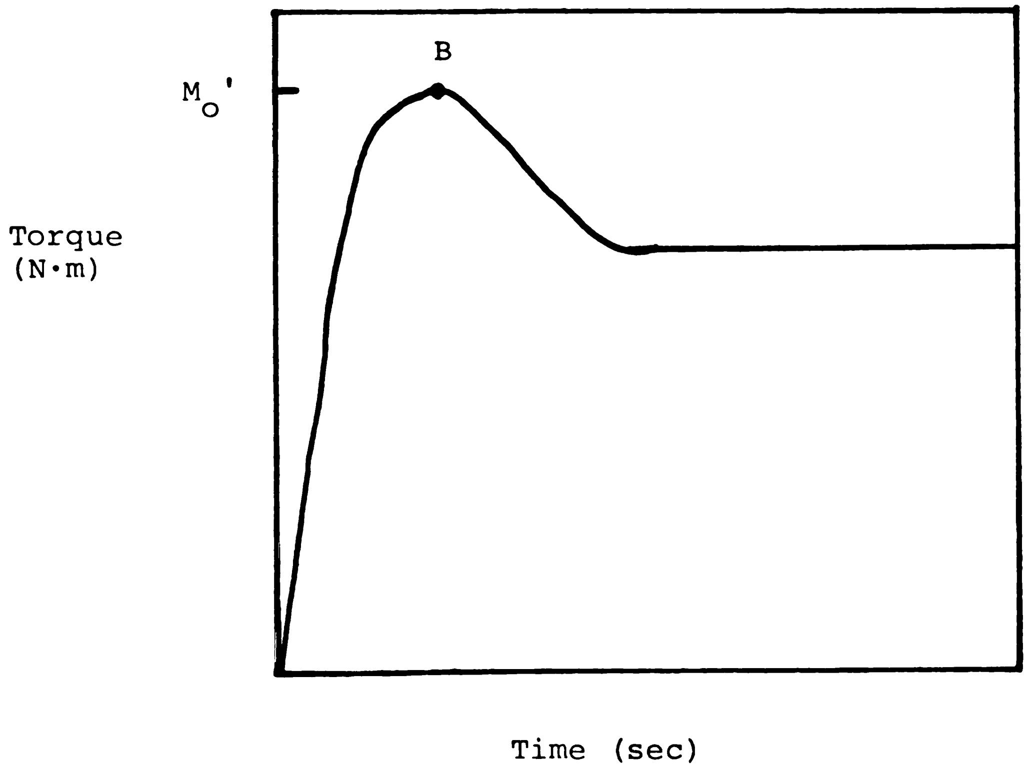

Figure 3. Yield stress determination using stress to initiate flow.

breakdown curve would retrace the first. A 60 minute recovery period was used with a second set of samples in case the rate of recovery was slower than the rate of breakdown. If no recovery was observed after either recovery period, irreversibility was assumed.

6.3. Paddle Mixer Costant (k') Data Collection and Analysis

The mixer constant, k', defined in Equation 13, was determined using standard solutions of hydroxypropyl methylcellulose, guar gum and corn syrup. The behavior of the standard fluids was evaluated using data acquired from the Haake RV-12 (measuring head M500 and sensor MVI) and using Equations 25 and 6 to calculate shear rate and shear stress, respectively. Power-law parameters, K and n, were calculated by linear regression analysis of the standard fluid shear stress/shear rate data (Table 5). A relatively slow angular velocity range (10-120 rpm) was chosen for the paddle mixer rheological parameter estimation test to simulate the rate of stirring of the apricot puree by the consumer. This, in turn, dictated that angular velocities within these limits be chosen for the determination of the standard fluids' flow curves.

In preliminary studies, the constant k' was shown not to be a function of angular velocity, but this will not be definite until further studies are completed. Therefore, the value of k' will be stated as "calculated at 60 rpm". Torque readings were taken with the Haake RV-12 and paddle mixer sensor at 60 rpm for all standard solutions.

To check the validity of Equation 13, a plot of log $(p/K\Omega^{n+1}d^3))$ versus (1-n) was prepared and found to be a straight line (Figure 4). The variable, p, was determined by multiplying 6.28 s^{-1} (60 rpm) by the torque reading generated by the paddle mixer. The slope of this plot is -log k'; therefore k' = 4.46. The actual data used to plot the curve are listed in Table 5.

6.4. Thixotropic Breakdown Data Collection and Analysis

As mentioned previously, a modified version of Tiu and Boger's method was used to characterize breakdown. Since the paddle mixer was used, only apparent shear stress and apparent shear rate could be calculated. Shear rate was calculated using Equation 13, where k' = 4.46, and shear stress was approximated using Equation 23, where τ_s/M_s was estimated as follows:

1) Using data from tests run on a standard fluid (Table 5), the value of τ_s was determined as:

$$\tau_s = K_s \, \dot{\gamma}^{n_s}$$

$$\tau_s = 4.93\ (6.28 \cdot 4.46)^{.292}$$

$$\tau_s = 13.056\ \mathrm{N \cdot m^{-2}}$$

where,

K_s, n_s and k' are taken from Table 5 (data on standard fluids)

2) $M_s = 0.001327$ N·m at angular velocity, 6.28 s^{-1} (Table 5).

3) Then, $\tau_s/M_s = 13.056/0.001327 = 9835$.

By substituting τ_s/M_s into Equation 23,

$$\tau_{a_x} = 9835\ M_x \tag{26}$$

The breakdown curves were run at constant velocity (20, 40, 60, 80, 100 and 120 rpm) for 10 minutes, and 51 data points were recorded for each curve. Only the first five points (0, 12, 24, 36 and 48 seconds) were used, since the curve, $1/(\eta_a-\eta_e)$ versus t, was nonlinear after this period of time. (Nonlinearity violates Equation 20.)

A plot of $1/(\eta_a-\eta_e)$ versus t, where $\eta = \tau_a/\dot{\gamma}_a$, was made and linearly regressed for each sample. The linear regression yielded a_1 and $(\frac{1}{\eta_{ao}-\eta_e})$, i.e. the slope and intercept, respectively (Equation 20). Then, a_1 was plotted against apparent shear rate, and the curve was linearly regressed.

The variable, b, was defined as the intercept, $1/(\eta_{ao}-\eta_e)$, from Equation 20. Since $\eta = \tau_a/\dot{\gamma}_a$,

$$b = \frac{1}{\frac{\tau_{ao}}{\dot{\gamma}_a} - \frac{\tau_e}{\dot{\gamma}_a}} \tag{27}$$

where,

τ_{ao} = approximated shear stress at time zero $(N\cdot m^{-2})$

Rearranging,

$$b = \frac{\dot{\gamma}_a}{\tau_{ao} - \tau_e} \tag{28}$$

By substituting shear rate and shear stress from Equations 13 and 26, respectively,

$$b = \frac{k'\Omega}{9835(M_o - M_e)} \qquad (29)$$

where,

M_e = torque at equilibrium (N·m)

M_o = torque at time zero (N·m)

Then, since k' = 4.46, as mentioned earlier,

$$b = \frac{4.46\Omega}{9835(M_o - M_e)} \qquad (30)$$

Solving for M_o yielded:

$$M_o = \frac{4.46\ \Omega}{9835\ b} + M_e \qquad (31)$$

thus, the initital torque, M_o, was estimated using the equilibrium torque, M_e, in Equation 31. The experimental torque at time zero taken from each breakdown curve was also used to estimate M_o for each set of data. The value of τ_{ao} in both cases was calculated using Equation 26. Then, each τ_{ao} was plotted against its respective $\dot{\gamma}_a$ to yield the values of K_o, n_o and τ_{y_o} by linear regression (Figure 8).

The equilibrium structural parameter, λ_e, was determined using Equation 21 and was tabulated (Table 7). The value of k_1 was calculated using Equation 19. Finally, the fluid's thixotropic behavior was characaterized by substituting the calculated values into Equations 15 and 16.

6.5. Wall Effect Data Collection and Analysis at Equilibrium

Using the MVI, MVII and MVIII sensors, equilibrium shear stress/shear rate data (10-120 rpm) were collected on samples previously degraded with the paddle mixer (10 minutes at 60 rpm). The three data sets obtained from the sensors were statistically compared using the student's t-value test for comparison of three linear equations (Kleinbaum and Kupper, 1978) (Table 4).

The null hypothesis, H_o, stated that slopes, n, calculated from MVI, MVII and MVIII data were the same and that the intercepts, ln K, were the same for all three data sets. Following is the model used in the statistical analysis:

$$y = \beta_o + \beta_1 I_1 + \beta_2 I_2 + \beta_3 X_3 + \beta_4 I_1 X_3 + \beta_5 I_2 X_3 \quad (32)$$

where,

I_1, I_2 = dummy variables

X_3 = ln (shear rate)

y = ln (shear stress)

$\beta_o, \beta_1, \beta_2, \beta_3, \beta_4, \beta_5$ = constants

since,

$$\tau = K\dot{\gamma}^n \qquad \ln \tau = \ln K + n \ln \dot{\gamma}$$

If the null hypothesis were true, $\beta_o = \beta_o + \beta_1 = \beta_o + \beta_2$ and $\beta_3 = \beta_3 + \beta_4 = \beta_3 + \beta_5$, which imply that $\beta_1 = \beta_2 = 0$ and $\beta_4 = \beta_5 = 0$, respectively. Thus, the null hypothesis assumed all β values were equal to zero. It follows that the t-values (corresponding to β values) either validated or invalidated the null hypothesis. Specifically, an absolute t-value greater than the tabulated value at the chosen level of significance implied that the constant, β_i, was statistically important and not equal to zero. At the

Table 4. Outline of statistics model used to check for wall effects.*

I_1	I_2	Equation	Data 1	Data 2
0	0	$y = \beta_o + \beta_3 X_3$	MVI	MVIII
0	1	$y = (\beta_o+\beta_2) + (\beta_3+\beta_5) X_3$	MVII	MVII
1	0	$y = (\beta_o+\beta_1) + (\beta_3+\beta_4) X_3$	MVIII	MVI

*Two computer runs were required for a complete analysis.

chosen level of significance, the three curves were determined to be the same or different using β values calculated in the statistical analysis.

6.6. Paddle Mixer Rheological Parameters Estimation

Torque/angular velocity data (10-120 rpm) were collected using the paddle mixer and Haake RV-12 with samples previously degraded. These data were linearly regressed after transformation using $y = ax^b$ as the model, where the constant, b, is the flow behavior index, n. The value of the consistency coefficient, K, was then calculated using Equation 14 with data taken at 60 rpm.

RESULTS AND DISCUSSION

7.1. Discussion of

7.1.1. Results of the Recovery Test

After running eight 10 minute and eight 60 minute recovery tests, it was determined that complete irreversibility was exhibited by the starch-thickened, strained apricot puree. (See Figure 5 for a representative sampling of curves.) Partial recovery may have occurred had the recovery period been extended to a few days. However, since a major reason for this study was to develop a quick method of quality control for industry, the storage of a sample over such a long recovery period seemed impractical. In addition, spoilage, which would change sample structure, could occur over an extended recovery period at ambient temperature.

7.1.2. Results of the Breakdown Analysis

As previously mentioned, a modified version of Tiu and Boger's (1974) method of breakdown characterization was used, where complete irreversibility was assumed and a paddle mixer was used instead of a concentric cylinder viscometer.

Following are the results of this study:

1. Figure 6 shows a plot of $1/(\eta_a - \eta_e)$ versus t for a representative sample at each angular velocity used in the breakdown analysis (20, 40, 60, 80, 100 and 120 rpm). The general trends of increasing slope, a_1, and intercept, $1/(\eta_{ao} - \eta_e)$, with increasing shear rate can be seen on this plot.

The increasing value of a_1 with increasing shear rate

Table 5. Data used to evaluate the mixer constant (k') for the MV paddle mixer.

Fluid	K(Pa-s^n)	n	$p=M\Omega(\frac{N-m}{s}x10^2)$	$\log(p/K\Omega^{n+1}d^3)$	1-n
Hydroxypropyl	16.55	.513	5.85	.489	.487
Methylcellulose	15.56	.520	5.73	.502	.479
2.5%	16.61	.505	5.77	.488	.494
	15.90	.513	5.62	.489	.486
Hydroxypropyl	7.29	.574	3.00	.508	.426
Methylcellulose	6.94	.586	3.11	.533	.413
2.0%	6.72	.588	3.06	.540	.411
	7.06	.576	3.08	.530	.423
Hydroxypropyl	2.10	.676	1.29	.597	.323
Methylcellulose	2.16	.672	1.27	.584	.327
1.5%	2.16	.675	1.30	.592	.324
	2.10	.680	1.29	.597	.319
Hydroxypropyl	1.84	.560	.724	.498	.439
Methylcellulose	1.26	.605	.583	.531	.394
1.0%	0.85	.683	.541	.612	.316
	1.83	.504	.626	.483	.495
Corn Syrup	2.70	1.00	4.88	.799	.000
	2.84	.992	4.74	.780	.008
	2.64	1.00	4.82	.814	.000
Guar Gum	30.98	.158	3.28	.248	.841
1.5%	31.65	.159	3.39	.253	.840
	27.39	.169	3.16	.278	.830
Guar Gum	7.28	.275	1.13	.319	.724
1.0%	*4.93	.292	.833	.345	.707
	7.99	.266	1.21	.316	.733
	8.62	.237	1.23	.315	.762
	10.76	.224	1.43	.293	.775

*data used in the shear stress approximation (Equation 26).

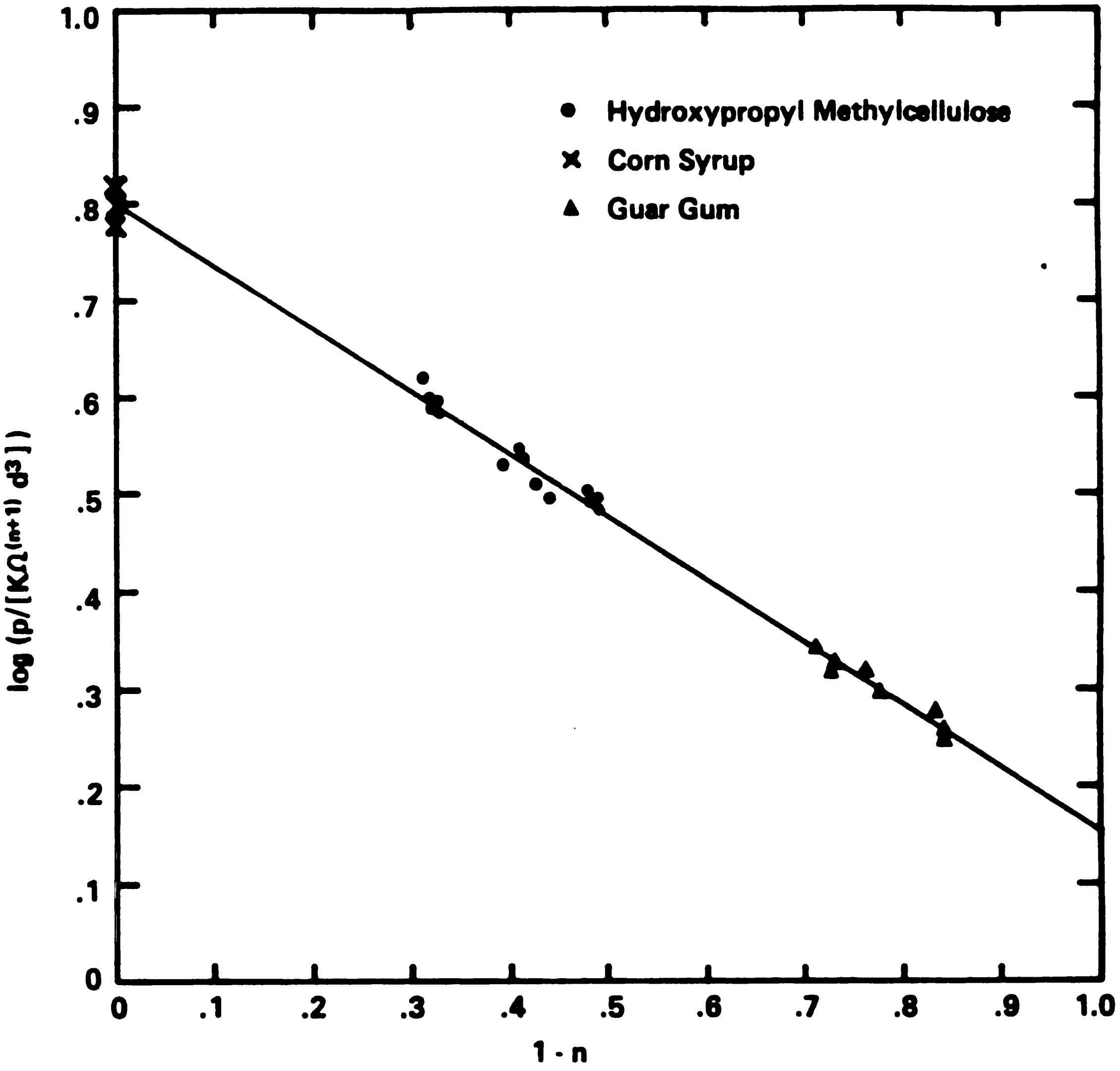

Figure 4. Plot used to evaluate the mixer viscometer constant (k) for the MV paddle.

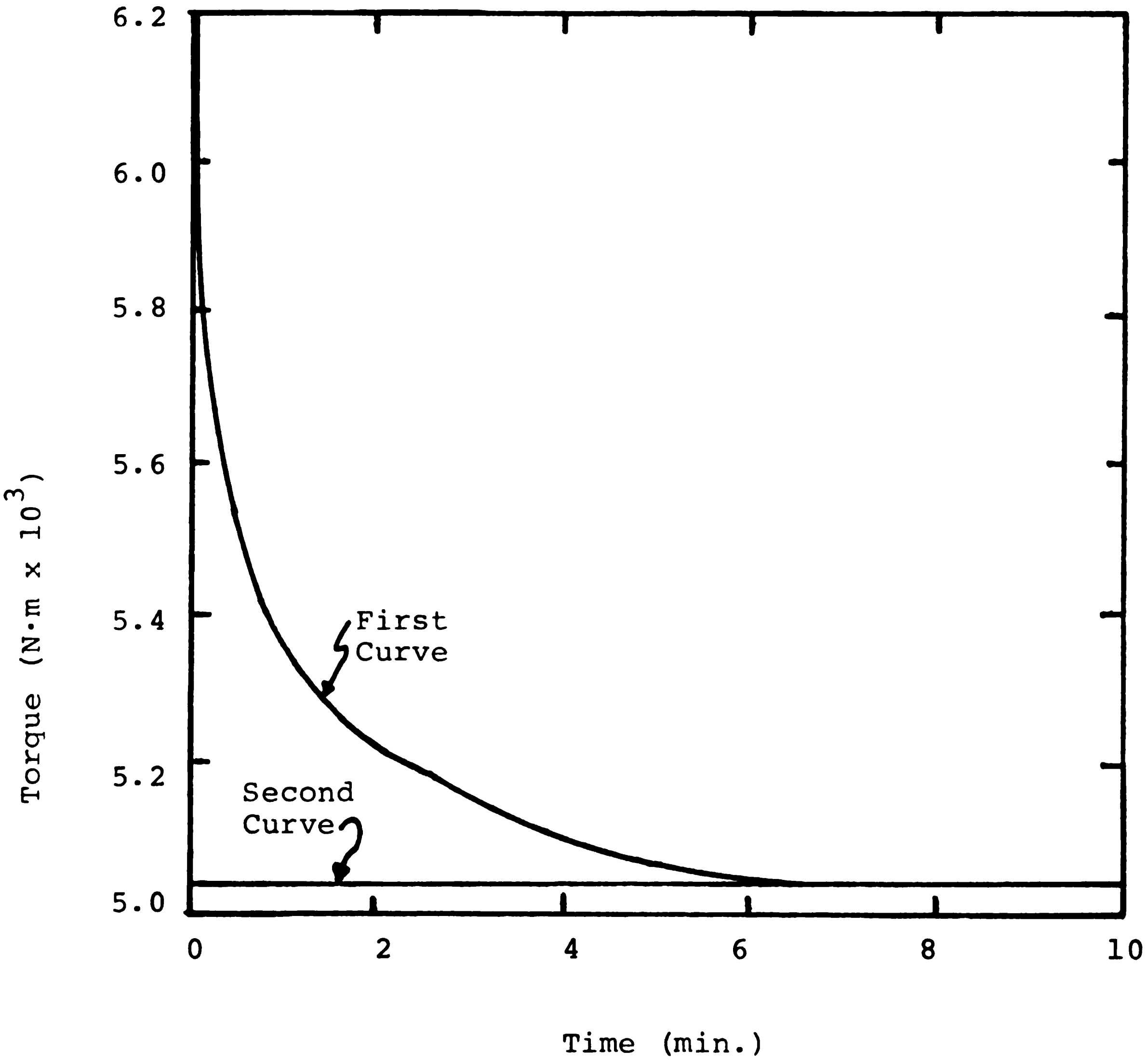

Figure 5. Recovery after a) 10 minutes.

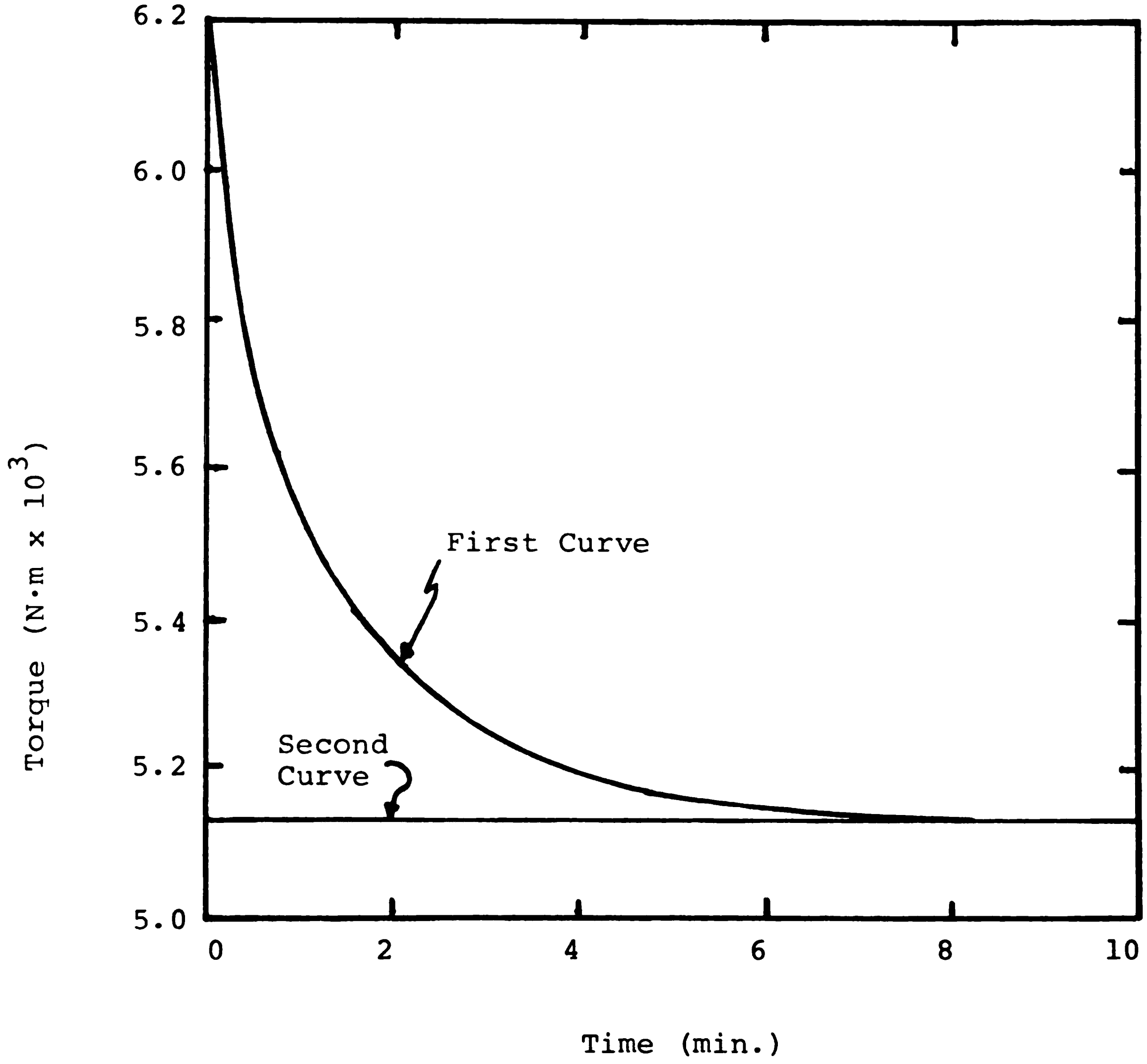

Figure 5. Recovery after b) 60 minutes.

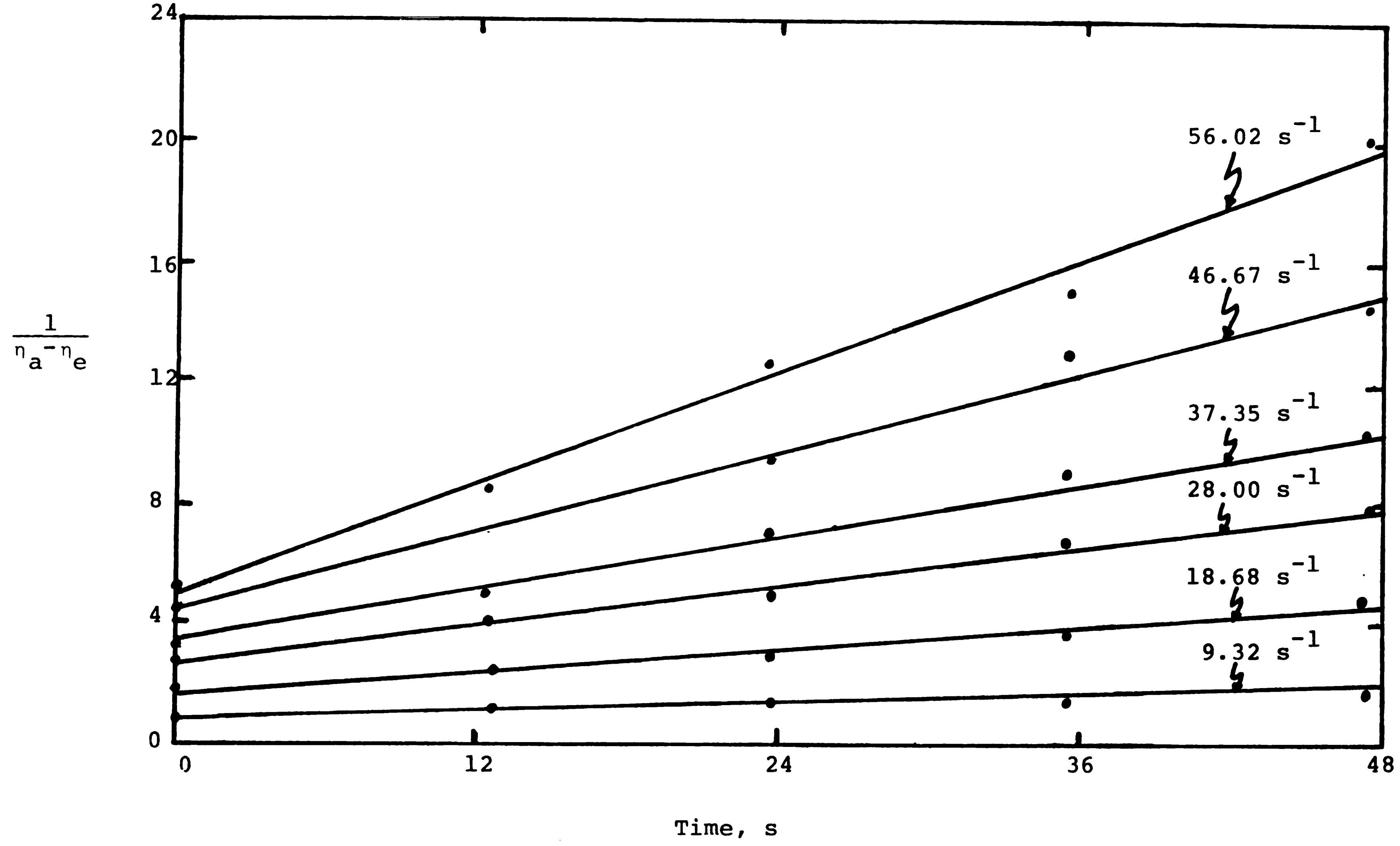

Figure 6. $1/(\eta_a-\eta_e)$ versus time at various shear rates.

shows that the rate of product structure breakdown is greater at higher shear rates. The increasing value of $1/(\eta_{ao}-\eta_e)$ with increasing shear rate is predictable since $1/(\eta_{ao}-\eta_e)$ becomes $\dot{\gamma}/(\tau_{ao}-\tau_e)$ using $\eta = \tau/\dot{\gamma}$. Specifically, $1/(\eta_{ao}-\eta_e)$ increases with increasing shear rate and decreasing $\tau_{ao}-\tau_e$; the increase in $1/(\eta_{ao}-\eta_e)$ is basically due to the increase in shear rate, while the proximity of the intercepts at different shear rates is due to the value of $\tau_{ao}-\tau_e$.

2. Figure 7 presents a_1 versus shear rate for each set of data in Table 6. a_1 $(\dot{\gamma})$ data was transformed and linearly regressed using $y = ax^b$, and the following relationship was found:

$$a_1 = .0526\ \dot{\gamma}^{1.443} \tag{33}$$

3. In Table 8 is the determination of τ_{y_o}, which was found to be 0.0 $N{\cdot}m^{-2}$, using the method outlined in section 6.1.1. (Yield Stress at Initial Point of Breakdown). Basically, Table 8 presents the results of a trial-and-error determination of τ_{y_o}. The data at time zero from the breakdown curves (Figure 8) were cross-plotted on a shear-stress-at-time-zero versus shear-rate plot, and linear regression was performed as follows: a) a value of τ_{y_o} was assumed, b) the data were linearly regressed, after transformation, using the assumed value of τ_{y_o}, c) r^2 and standard deviation were tabulated, d) steps a through c were repeated for different assumed values of τ_{y_o}.

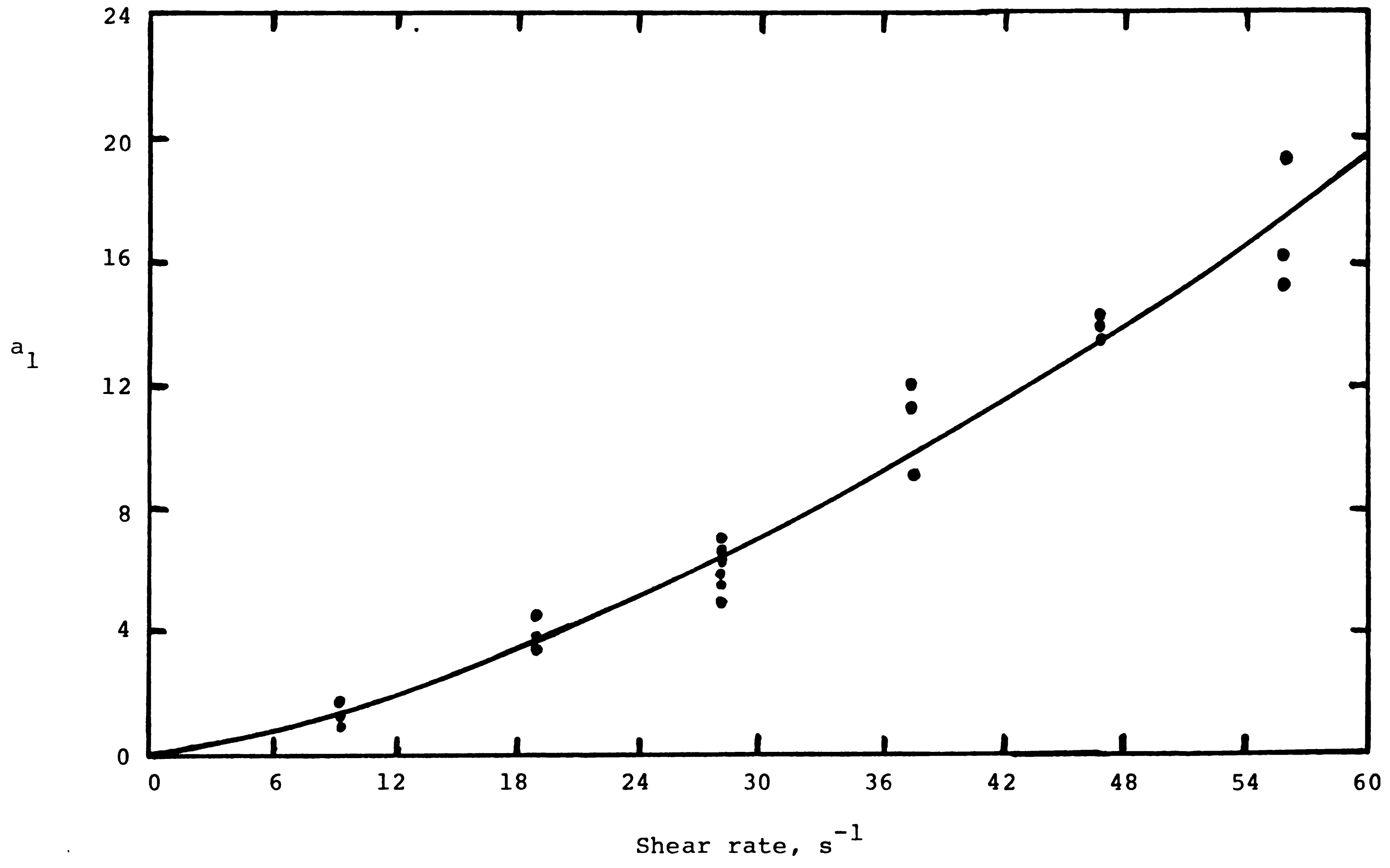

Figure 7. a_1 versus shear rate.

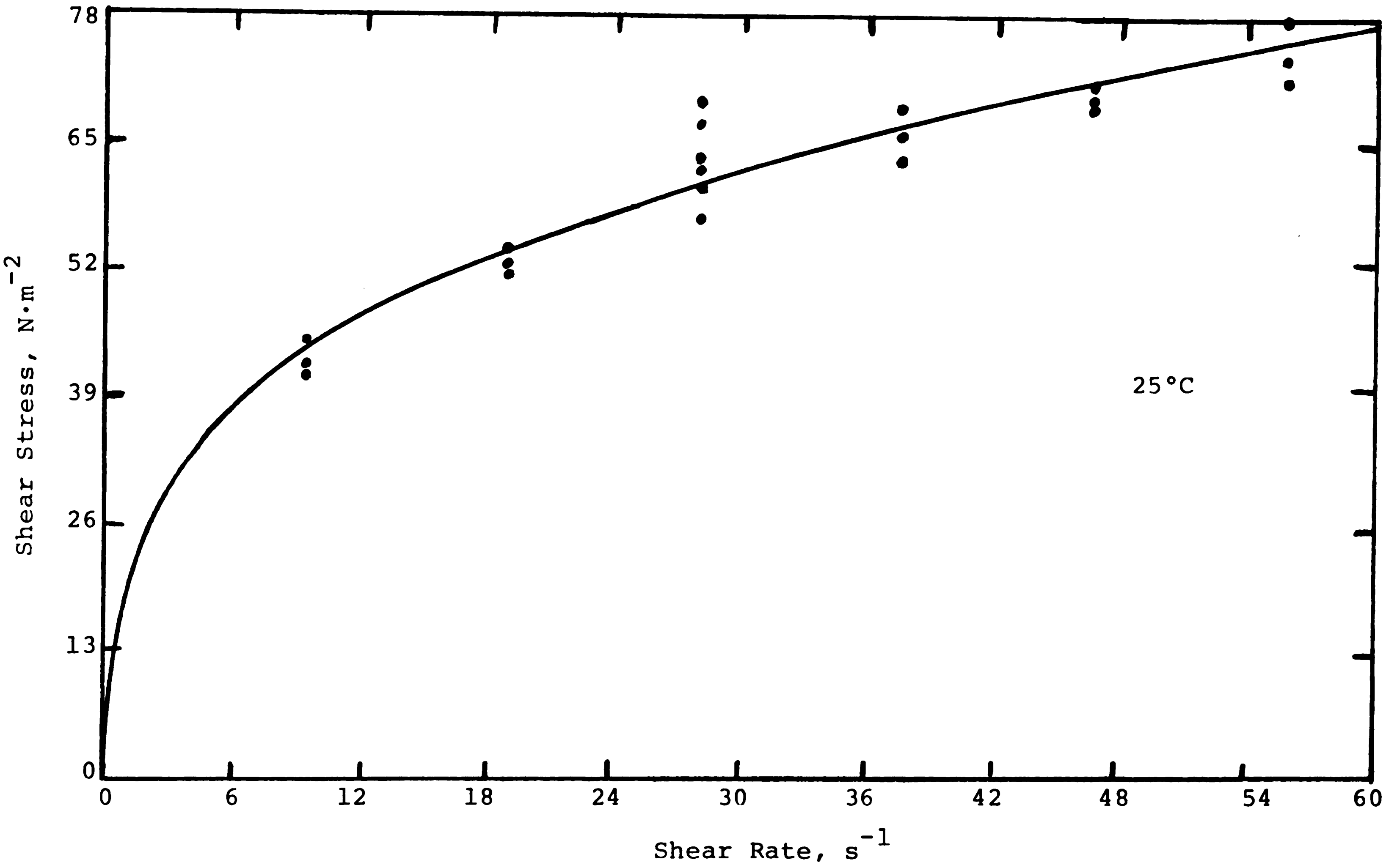

Figure 8. Rheogram obtained at time zero from modified Tiu and Boger analysis using the MV paddle mixer.

Table 6. Experimental values of a_1 and $1/(\eta_a-\eta_e)$ data obtained using the modified Tiu and Boger method.

Sample (rpm)	Slope a_1	Intercept $1/(\eta_{ao}-\eta_e)$	Number of Points	Shear Rate $\dot{\gamma}_a$ (s^{-1})
1 (20)	1.578	.948	5	9.315
2 (20)	1.122	.864	6	9.315
3 (20)	1.241	.940	5	9.315
1 (40)	4.384	1.719	5	18.675
2 (40)	3.543	1.745	5	18.675
3 (40)	3.747	1.786	6	18.675
1 (60)	6.341	1.614	5	28.000
2 (60)	7.089	2.824	5	28.000
3 (60)	4.819	2.352	5	28.000
4 (60)	6.326	2.859	5	28.000
5 (60)	5.693	2.375	5	28.000
6 (60)	6.585	3.015	5	28.000
7 (60)	5.660	2.753	5	28.000
1 (80)	12.086	3.944	5	37.350
2 (80)	11.285	2.904	6	37.350
3 (80)	9.059	3.457	5	37.350
1(100)	13.540	4.547	5	46.665
2(100)	14.156	4.592	5	46.665
3(100)	14.025	4.720	5	46.665
1(120	19.32	6.092	6	56.024
2(120)	16.23	5.695	6	56.024
3(120)	15.33	5.294	5	56.024

Table 7. Torque at time zero data and structural parameter data obtained using the modified Tiu and Boger method.

	Theoretical Data			Actual Data		
Sample (rpm)	M_e $(N\cdot m x 10^3)$	M_o $(N\cdot m x 10^3)$	τ_{ao} (N/m^2)	M_o $(N\cdot m x 10^3)$	τ_{ao} (N/m^2)	λ_e
1 (20)	3.22	4.22	41.50	4.24	41.66	.725
2 (20)	3.46	4.56	44.85	4.62	45.42	.779
3 (20)	3.28	4.29	42.19	4.35	42.79	.739
1 (40)	4.20	5.30	52.13	5.24	51.55	.764
2 (40)	4.43	5.52	54.29	5.47	53.82	.806
3 (40)	4.23	5.29	52.03	5.29	52.03	.770
1 (60)	5.31	7.07	69.53	6.30	61.97	.853
2 (60)	5.43	6.44	63.34	6.48	63.70	.872
3 (60)	5.63	6.84	67.27	6.85	67.37	.904
4 (60)	5.31	6.31	62.06	6.36	62.58	.853
5 (60)	5.64	6.84	67.27	6.88	67.66	.906
6 (60)	4.87	5.81	57.14	5.85	57.57	.782
7 (60)	5.12	6.15	60.49	6.20	60.96	.823
1 (80)	5.43	6.39	62.85	6.36	62.59	.798
2 (80)	5.65	6.96	68.45	6.81	67.01	.831
3 (80)	5.60	6.70	65.87	6.70	65.90	.823
1(100)	5.97	7.01	68.97	7.04	69.22	.820
2(100)	6.03	7.06	69.44	7.05	69.32	.828
3(100)	6.20	7.21	70.91	7.18	70.64	.851
1(120)	6.52	7.46	73.32	7.53	74.01	.847
2(120)	6.28	7.28	71.60	7.39	72.68	.815
3(120)	6.86	7.94	78.09	7.99	78.57	.891

Table 8. Series of data and calculations* used to determine yield stress at time zero.

Assumed yield stress τ_{y_o} (N·m^{-2})	K_o (Pa·s^n)	n_o	R^2	σ (std. dev.)
20	8.146	0.482	0.9110	0.2831
15	11.26	0.421	0.9119	0.2471
9	15.34	0.366	0.9122	0.2148
8	16.05	8.358	0.9123	0.2103
7	16.77	0.351	0.9123	0.2059
6	17.50	0.344	0.9123	0.2017
5	18.24	0.337	0.9123	0.1977
4	18.98	0.330	0.9123	0.1939
3	19.73	0.324	0.9123	0.1902
2	20.48	0.318	0.9122	0.1866
1	21.24	0.312	0.9122	0.1832
0	22.01	0.307	0.9122	0.1799

*using the following model for linear regression:

$$y = ax^b + c$$

$$\ln (y-c) = \ln a + b\ln X$$

where y = shear stress data

x = shear rate data

The best approximation of τ_{y_o} was taken from the curve with the lowest standard deviation, σ.

4. Figure 8 shows a plot of shear stress/shear rate data at time zero from Tables 7 and 6, respectively. By linear regression of the transformed data, shear stress and shear rate were found to be related by

$$\tau_{ao} = 22.01\ \dot{\gamma}_a^{.307} \tag{34}$$

where,

$K_o = 22.01\ Pa \cdot s^n$

$n_o = 0.307$

$\tau_{y_o} = 0.0\ N \cdot m^{-2}$

This linear regression is the best fitting curve from the τ_{y_o} approximation above (Table 8).

5. By substituting a_1 from Equation 33 and K_o, n_o and τ_{y_o} from Equation 34 into Equation 19, $k_1\ (\dot{\gamma})$ was determined as

$$k_1 = 1.158\ \dot{\gamma}_a^{.750} \tag{35}$$

6. λ_e was determined for every sample using Equation 21 (Table 7) and the average value was:

$$\lambda_e = 0.822$$

7. The calculated constants were then substituted into the phenomenological relationship and the rate equation, respectively, as

$$\tau = \lambda\ (22.01\ \dot{\gamma}^{.307}) \tag{36}$$

$$\frac{d\lambda}{dt} = -\ (1.158\dot{\gamma}^{.750})(\lambda-0.822)^2 \tag{37}$$

Equations 36 and 37 completely characterize breakdown, although it must be noted that the sample is irreversible. It can be seen in Equation 37 that $d\lambda/dt$ is a function of $\dot{\gamma}_a$ and λ. Since $\dot{\gamma}$ is held constant during any given breakdown in Tiu and Boger's analysis, only λ changes with time. At the initital point of breakdown, $d\lambda/dt$ is at its greatest value. Since $\lambda = 1$ at time zero and approaches 0.822 at equilibrium, the value of $\lambda - \lambda_e$ in Equation 37 decreases with time, i.e. $d\lambda/dt$ decreases with time. This, in turn, predicts the actual decrease in rate of breakdown as the structure approaches equilibrium (Figure 5).

By integrating Equation 37 from $\lambda = 1$ at $t = 0$ to $\lambda = \lambda$ at $t = t$ a relationship between λ and t may be found as

$$\lambda\ (t) = (1.158\ \dot{\gamma}^{.750} + 5.62)^{-1} + 0.822 \qquad (38)$$

Thus, by substituting Equation 38 into Equation 36 the actual shear stress/shear rate relationship at any time, t, can be determined.

This method of characterization is an excellent way of mathematically describing irreversible breakdown because it is simple and complete; there are two areas which need improvement, however. The simple analysis of yield stress chosen for this study could yield only an approximate value and depended greatly on the computer software used to do the curve fitting. Also, transfer of sample from the jar into the MV cup resulted in sample breakdown prior to breakdown under controlled conditions.

The problem of loading shear breakdown during loading of the cup into the viscometer was minimized by using the paddle mixer. The replacement of the concentric cylinder viscometer with the paddle mixer also eliminated the possibility of erroneously assuming a decrease in torque at constant shear rate due to wall effects, i.e. thinning of sample near the bob, was thixotropic breakdown. (The mixer maintained the sample suspension.)

7.1.3. Results of Wall Effect Analysis

Yield stress at equilibrium was found to be zero by both methods presented in section 6.1.2. (Yield Stress at Equilibrium). The shear stress/shear rate equations for the three sensors were

$$\text{MVI:} \quad \tau = 12.34\, \dot{\gamma}^{.418} \tag{39}$$

$$\text{MVII:} \quad \tau = 16.25\, \dot{\gamma}^{.362} \tag{40}$$

$$\text{MVIII:} \quad \tau = 18.80\, \dot{\gamma}^{.333} \tag{41}$$

(Table 11).

The three curves were found to be statistically different at the 99.9% confidence level (Table 9). Table 10 lists the rheological parameters for Karo light corn syrup obtained using the MVI, MVII and MVIII sensors. Since the corn syrup, which is considered homogeneous, had nearly equal rheological parameters for all three sensors, there was no sign of wall effects occuring. The Karo syrup test confirmed that the differences in apricot puree rheological data were due to wall effects and not to inherent problems with the viscometer.

Table 9. The β constants determined using the statistical model.

Constant	Value	Standard Error	t-value
TEST 1 on Apricot puree			
β_o	2.513	0.180 x10-1	139.55
β_1	0.421	0.226 x10-	18.63
β_2	0.275	0.234 x10-1	11.78
β_3	0.418	0.376 x10-2	111.10
β_4	-0.0846	0.536 x10-2	-15.78
β_5	-0.0554	0.529 x10-2	-10.47
TEST 2 on Apricot puree			
β_o	2.934	0.137 x10-1	214.77
β_1	-0.421	0.226 x10-1	-18.63
β_2	-0.146	0.202 x10-1	- 7.22
β_3	0.333	0.382 x10-2	87.15
β_4	0.0846	0.536 x10-2	15.78
β_5	0.0292	0.534 x10-2	5.48

Table 10. Rheological data for Karo light corn syrup.

Sensor	n	K (Pa·s^n)
MVI	1.0	2.46
MVII	1.0	2.31
MVII	1.0	2.39
MV Paddle	1.0	2.47

Table 11. Rheological parameters of starch-thickened, strained apricots obtained using various MV sensors and the MV paddle mixer.

Sensor	K(Pa-sn)	n	r^2	data points
MVI: Test 1	12.13	.420	.999	13
Test 2	12.15	.422	.999	13
Test 3	12.21	.420	.998	13
Test 4	12.35	.419	.998	13
Test 5	12.41	.424	.998	13
Test 6	12.27	.420	.997	13
Test 7	12.97	.411	.996	12
Test 8	13.44	.403	.998	13
Test 9	12.04	.417	.999	13
Test 10	12.12	.422	.997	13
Pooled Data	12.34	.418	.995	129
NVII: Test 1	15.91	.370	.997	13
Test 2	16.10	.361	.997	13
Test 3	16.75	.366	.997	13
Test 4	17.25	.352	.997	13
Test 5	16.46	.371	.997	13
Test 6	17.28	.362	.997	13
Test 7	16.37	.357	.998	13
Test 8	16.96	.354	.998	13
Test 9	14.69	.368	.998	13
Test 10	14.92	.364	.998	13
Pooled Data	16.25	.362	.980	130
MVIII: Test 1	17.47	.348	.995	12
Test 2	16.31	.370	.984	13
Test 3	19.32	.330	.993	13
Test 4	18.94	.337	.995	12
Test 5	19.23	.329	.993	12
Test 6	19.51	.329	.994	13
Test 7	20.03	.326	.995	13
Test 8	18.98	.335	.993	13
Test 9	17.97	.335	.995	13
Test 10	18.93	.319	.991	13
Pooled Data	18.80	.333	.984	127
Paddle Test 1	14.04	.380	.995	13
Test 2	14.63	.378	.996	13
Test 3	14.08	.381	.998	13
Test 4	14.92	.367	.997	12
Test 5	13.70	.381	.997	13
Test 6	14.76	.371	.998	13
Test 7	13.59	.378	.998	13
Test 8	13.73	.379	.997	13
Pooled Data	14.17	.377	.992	103

The plots of Equations 39, 40 and 41 are shown in Figure 9. K and n from Equations 39, 40 and 41 were used to calculate apparent viscosity in $\eta_a = K\dot{\gamma}^{n-1}$, and η_a was plotted as a function of shear rate in Figure 10. In the basic rheogram (Figure 9), there is a marked difference in the three curves, while in Figure 10, the three curves seem to converge at higher shear rates. One would expect Figures 9 and 10 to show the same results. However, K and n are not independent of each other; thus the rearrangement of variables in the three equations can alter the relationships of the latter. Therefore, although the apparent viscosities were the same, for all practical purposes, the rheograms were statistically different and therefore, there was a wall effect.

7.1.4. Results of Paddle Mixer Test

The paddle mixer was used to approximate the equilibrium structure of the apricot puree, in case wall effects were indeed occuring with the concentric cylinder viscometer. The following shear stress/shear rate relationship was estimated (Table 11):

$$\tau = 14.17\,\dot{\gamma}^{.377} \qquad (41)$$

Figures 9 and 10 illustrate the accuracy of the paddle mixer approximation in comparison to the MVI, MVII and MVIII curves. Since the paddle mixer keeps the sample suspended, one would expect the paddle mixer curve to be higher than the other curves on the plot, due to lack of wall effects. However, for reasons not yet understood, this is not the

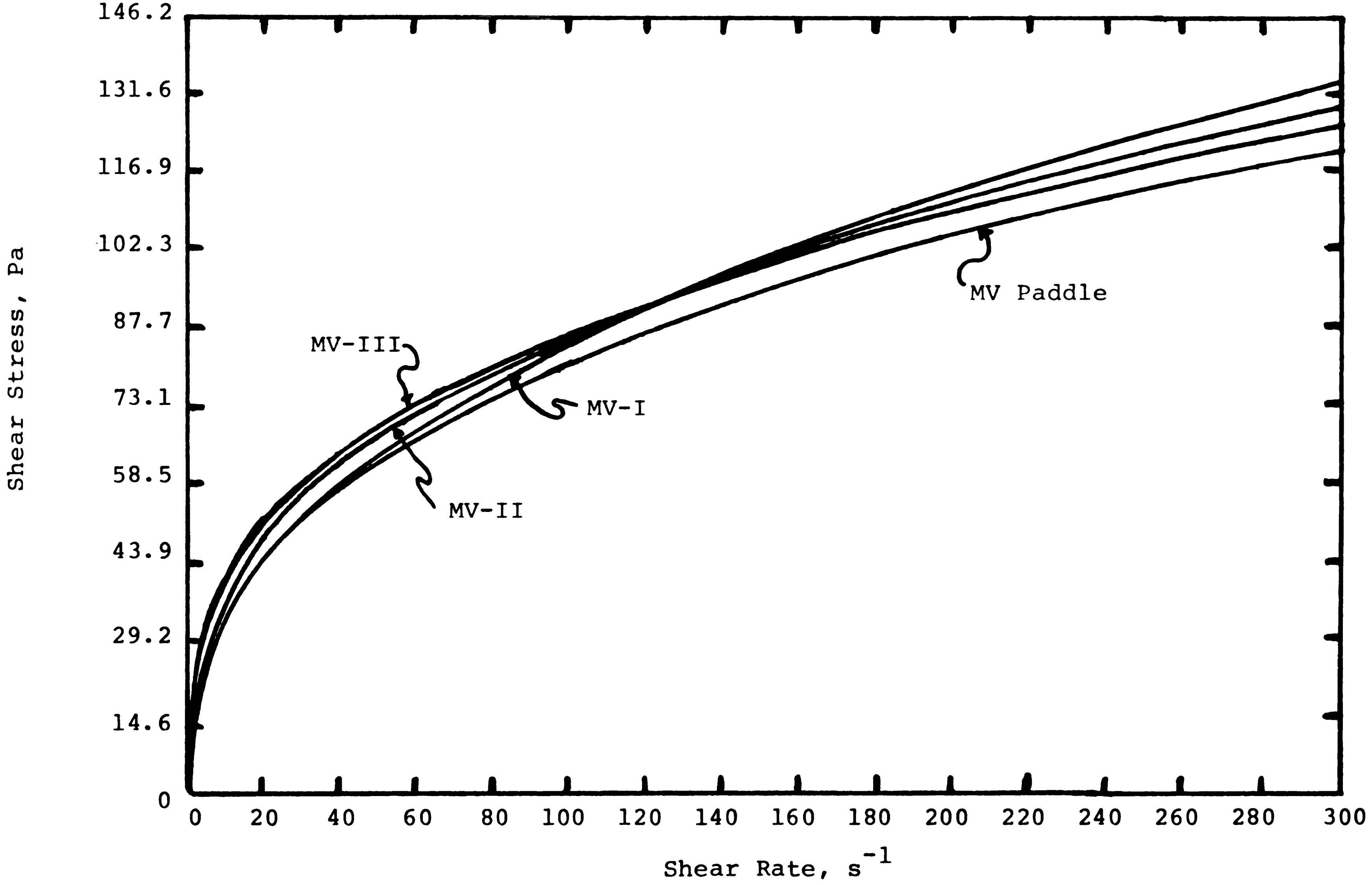

Figure 9. Rheograms obtained using the various MV sensor and the MV paddle mixer.

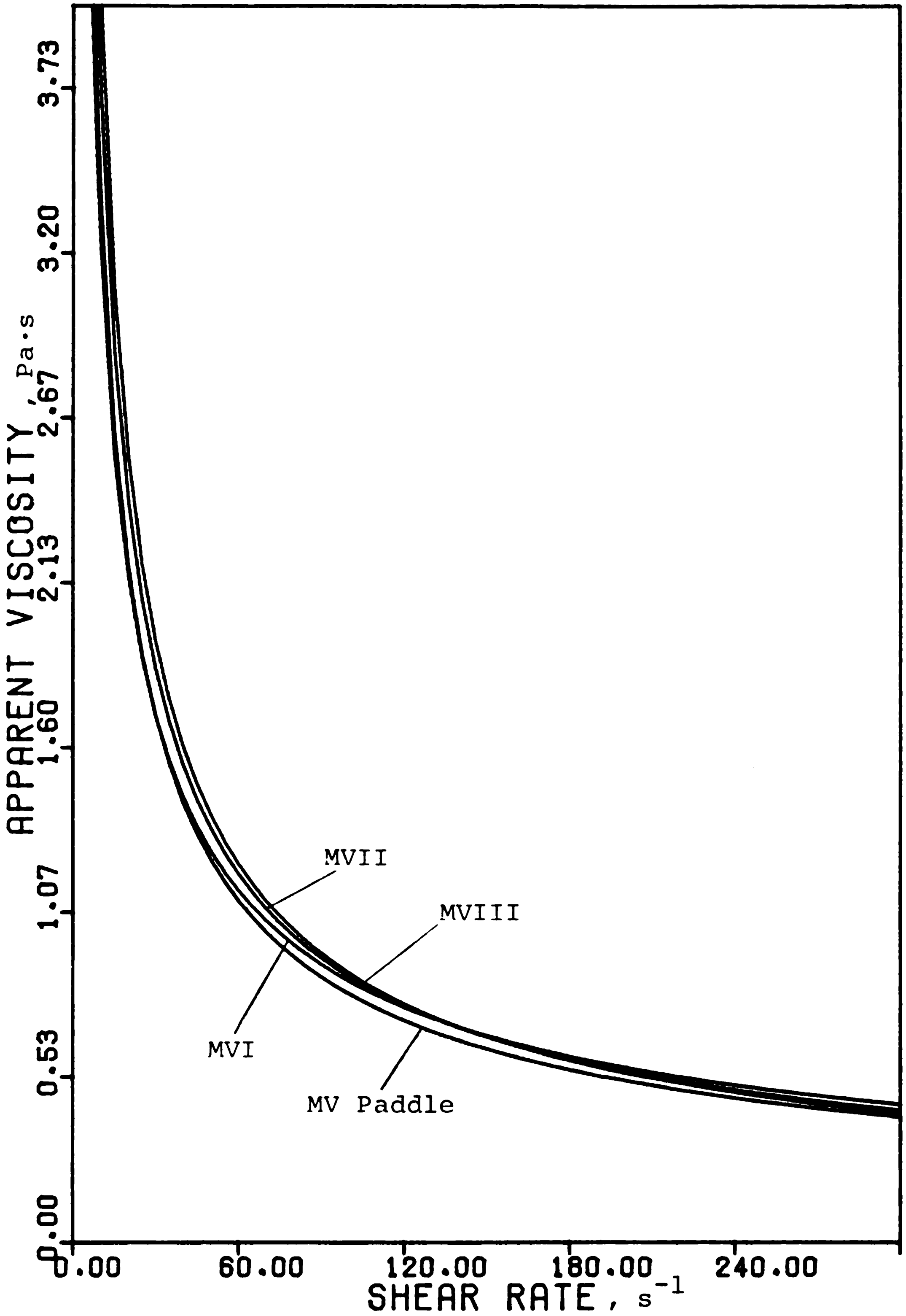

Figure 10. Apparent viscosity versus shear rate obtained using various MV sensors and the MV paddle mixer.

case. Note that laminar flow is present since Re = 0.002 using K and n from Equation 41.

7.1.5. Relationship Between Phenomenological Relationship and Equilibrium Rheogram

The phenomenological relationship used in the breakdown structure analysis (Equation 36) should be the same as the equilibrium rheogram (Equation 41) when the equilibrium structural parameter is substituted into Equation 36.

The structural parameter, λ, at equilibrium is equal to 0.822. Thus, Equation 36 becomes

$$\tau = 18.09\ \dot{\gamma}_a^{.307} \qquad (42)$$

and Equation 41, the equilibrium rheogram, is

$$\tau = 14.17\,\dot{\gamma}_a^{.377}$$

As previously discussed in Section 7.1.3., K and n are not independent variables. Thus, even though Equations 42 and 41 are different, their respective apparent viscosities may be similar enough, especially at higher shear rates, and the structure characterized by the two equations may be equal, as expected. Apparent viscosity ($\eta_a = K\dot{\gamma}^{n-1}$) versus shear rate was plotted for each equation (Figure 11). The two curves show the same basic structure, especially at higher shear rates, and therefore, satisfy the assumption that the equilibrium structure can be characterized by both the breakdown analysis and the equilibrium analysis. Slight differences may be due to a small, but undetected, yield stress.

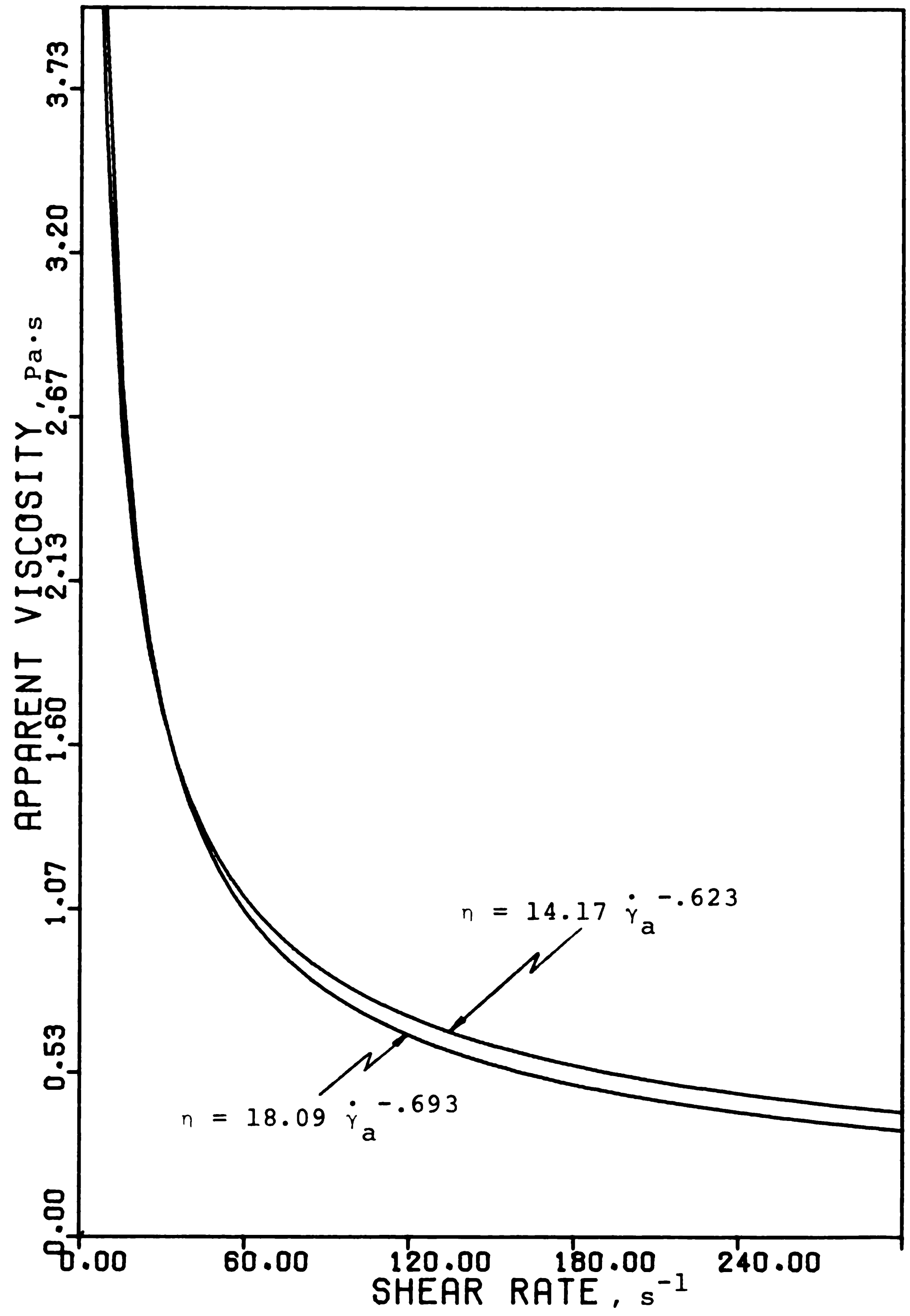

Figure 11. Apparent viscosity versus shear rate obtained from phenomenological relationship at equilibrium and equilibrium rheogram.

CONCLUSIONS

It was shown that a paddle mixer could be used in the rheological analysis of starch-thickened, strained apricot puree.

A complete rheological analysis was performed on the product and the following conclusions are supported:

1. The product showed completely irreversible breakdown.
2. The breakdown curve analysis gave the following relationships:
    a. Phenomenological Relationship: $\tau = (22.01\ \dot{\gamma}_a^{.307})$
    b. Rate equation: $\frac{d\lambda}{dt} = -(1.158\ \dot{\gamma}^{.750})\ (\lambda - .822)^2$
3. Wall effects did occur with the concentric cylinder viscometer.
4. The equilibrium structure rheogram of the product was determined using the paddle mixer as $\tau = 14.17\ \dot{\gamma}_a^{.377}$

SUGGESTIONS FOR FURTHER STUDY

1) One possible way to eliminate breakdown during loading of sample into the cup is to replace the MV cup with the jar in which the product is packaged. Further study is necessary to devise such a system.

2) It would be valuable to determine whether or not k' is a function of the angular velocity used to calculate it.

3) Further investigation into improving methods of yield stress determination is greatly encouraged, since only simple estimates of yield stress could be performed in this study.

4) It was impossible to completely characterize wall effects in this study. The viscometer used did not conform to the geoemtry required by Mooney's method, nor could it yield the angular velocities required to yield the same torque for all three sensors required by both Oldroyd's and Mooney's methods. Wall effect characterization studies are suggested.

5) It would be interesting to do a study on viscous heating during rotation of the sensor and the possible effects this heating would have on the highly temperature-dependent rheological properties.

6) Finally, it would be beneficial to further studies if it were confirmed the λ_e is independent of shear rate.

LIST OF REFERENCES

REFERENCES

1. Canovas, G.V.B. and Peleg, M. 1983. Flow parameters of selected commercial semi-liquid food products. Journal of Texture Stud. 14:213.

2. Charm, S.E. 1962. The nature of role of fluid consistancy in food engineering applications. Adv. Food Res. 11:356.

3. Cheng, D.C.-H. and Evans, F. 1965. Phenomenological characaterization of the rheological behaviour of inelastic reversible thixotropic and anti-thixotropic fluids. British J. Appl. Phys. 16:1599.

4. Dekee, D., Turcotte, G. and Fildey, K. 1980. New method for the determination of yield stress. J. of Texture Stud. 10:281.

5. Dickie, A.M. and Kokini, J.L. 1982. Use of the Bird-Leider equation in food rheology. J. of Food Process Engineering. 5:157.

6. Dickie, A.M. and Kokini, J.L. 1983. An improved model for food thickness from non-Newtonian fluid mechanics in the mouth. J. of Food Science. 48:57.

7. Duran, L. and Costell, E. 1982. Rheology of apricot puree: characterization of flow. J. of Texture Stud. 13:43.

8. Evans, I.D. and Haisman, D.R. 1980. Rheology of gelatinized starch suspensions. J. of Texture Stud. 10:347.

9. Fennema, O.R. 1976. Principles of Food Science: Part 1 Food Chemistry. Marcel Dekker, Inc. New York, New York, pp. 105-106.

10. Green, H. and Weltman, R.N. 1943. Analysis of the thixotropy of pigment-vehicle suspensions. Industrial and Engineering Chem. 15:201.

11. Hahn, S.J., Ree, T. and Eyring, H. 1959. Flow mechanism of thixotropic substances. Industrial and Engineering Chem. 51:856.

12. Harper, J.C. 1960. Viscometric behavior in relation to evaporation of fruit purees. Food Tech. 14:557.

13. Harris, J. 1967. A continuum theory of time-dependent inelastic flow. Rheol. Acta. 6:6.

14. Heywood, N.I. 1981. The measurement of thixotropic properties. Lecture Numer 9. Warren Spring Laboratory.

15. Howling, D. 1980. The influence of the structure of starch on its rheological properties. Food Chemistry. 6:51.

16. Kemblowski, Z., and Petera, J. 1979. Rheological characterization of thixotropic fluids. Rheological Acta. 18:702.

17. Kemblowski, Z., and Petera, J. 1980. A generalized rheological model of thixotropic materials. Rheological Acta. 19:529.

18. Krieger, I.M. 1968. Shear rate in the Couette viscometer. Trans. of Soc. of Rheol. 12:5.

19. Lang, E.R. and Rha, C. 1981. Determination of yield stresses of hydrocolloid dispersions. J. of Texture Stud. 12:47.

20. Metzner, A.B. and Otto, R.E. 1957. Agitation of non-Newtonian fluids. Am. Inst. Chem. Engrs. 3:1.

21. Mooney, M. 1931. J. of Rheol. 2:210.

22. Oldroyd, J.G. 1956. Rheology: Theory and Applications Vol. I (edited by F.R. Eirich). Academic Press. New York. pp. 653-682.

23. Petrellis, N.C. and Flummerfelt, R.W. 1973. Rheological behavior of shear degradable oils: kinetic and equilibrium properties. Canadian J. of Chemical Engineering. 51:291.

24. Rao, M.A. 1975. Measurement of flow properties of food suspensions with a mixer. J. of Texture Stud. 6:533.

25. Rao, M.A. and Otoya Palomino, L.N. 1974. Flow properties of tropical fruit purees. Food Tech. 39:160.

26. Rieger, F. and Novak, V. 1973. Power consumption of agitators in highly viscous non-Newtonian liquids. Trans. Instn. Chem. Engrs. 51:105.

27. Saravacos, G.D. 1968. Tube viscometry of fruit purees of fruit juices. Food Tech. 22:89.

28. Saravacos, G.D. and Moyer, J.C. 1967. Heating rates of fruit products in an agitated kettle. Food Tech. 21:372.

29. Schoch, T.J. 1969. Carbohydrates and their Roles. (edited by Schultz, H.W., Cain, R.F. and Wrolstad, R.W.). AVI Publishing Co. Westport, CT. pp. 395-417.

30. Sheth, B.B. 1976. Viscosity measurements and interpretation of viscosity data. J. of Texture Stud. 7:157.

31. Steffe, J.F., Mohamed, I.O. and Ford, E.W. 1983. Rheological properties of fluid foods. American Society of Agricultural Engineers, paper number 83-6512. St. Joseph, MI.

32. Steffe, J.F., Mohamed, I.O. and Ford, E.W. 1984. Pressure drop across valves and fittings for pseudoplastic fluid in laminar flow. Trans. of ASAE. 27:616.

33. Tiu, C. and Boger, D.V. 1974. Complete rheological characterization of time-dependent food products. J. of Texture Stud. 5:329.

34. Van Wazer, J.R., Lyons, J.W., Kim, K.Y. and Colwell, R.E. 1963. Viscosity and Flow Meaurement: A Laboratory Handbook of Rheology. John Wiley and Sons, Inc. USA.

35. Vacadlo, J.J. and Charles, M.E. 1971. Measurement of yield stress of fluid-like viscoplastic substances. Canadian J. of Chem. Eng. 49:576.

36. Watson, E.L. 1968. Rheological behavior of apricot purees and concentrate. Canadian Agric. Eng. 10:8.

37. Whorlow, R.W. 1980. Rheological Techniques. Ellis Horword Limited. West Sussex, England. pp. 155-157.

38. Woodman, M. and Marsden, A. 1966. Rheological investigation of a thixotropic lotion. J. Pharm. Pharmac. 18:198S.

APPENDICES

APPENDIX A

ANALYSIS OF STABILITY OF STARCH

APPENDIX A

ANALYSIS OF STABILITY OF STARCH

The plot that follows is a representation of the stability of the starch used in the analysis. Three different combinations of starch were used and the speed of breakdown determined as a slope of the breakdown curve, as characterized by $M = a + b \ln t$ where M = torque, a = intercept and b = slope. The product used in the thesis is Batch 3 on this plot. The slight change in slope seen in Batch 3 in the first days of the study as opposed to Batches 1 and 2 shows the relative stability of the product. Batches 1 and 2 also showed synersis problems over time while Batch 3 did not.

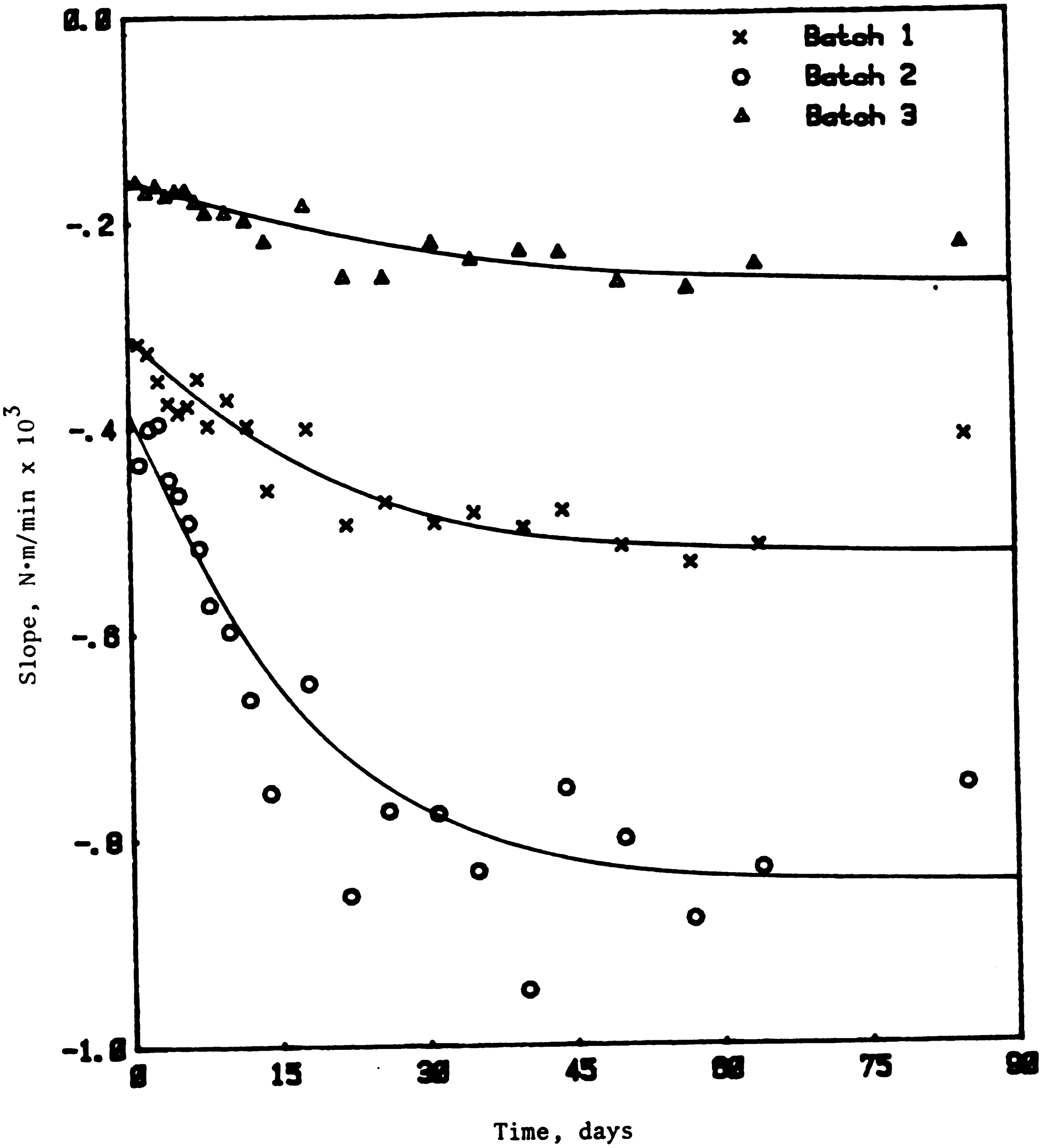
0.0
-.2
-.4
-.6
-.8
-1.0
0
15
30
45
60
75
90
Slope, N·m/min x 10^3
Time, days
× Batch 1
o Batch 2
▲ Batch 3

APPENDIX B

FLOW CHART OF ANALYSIS

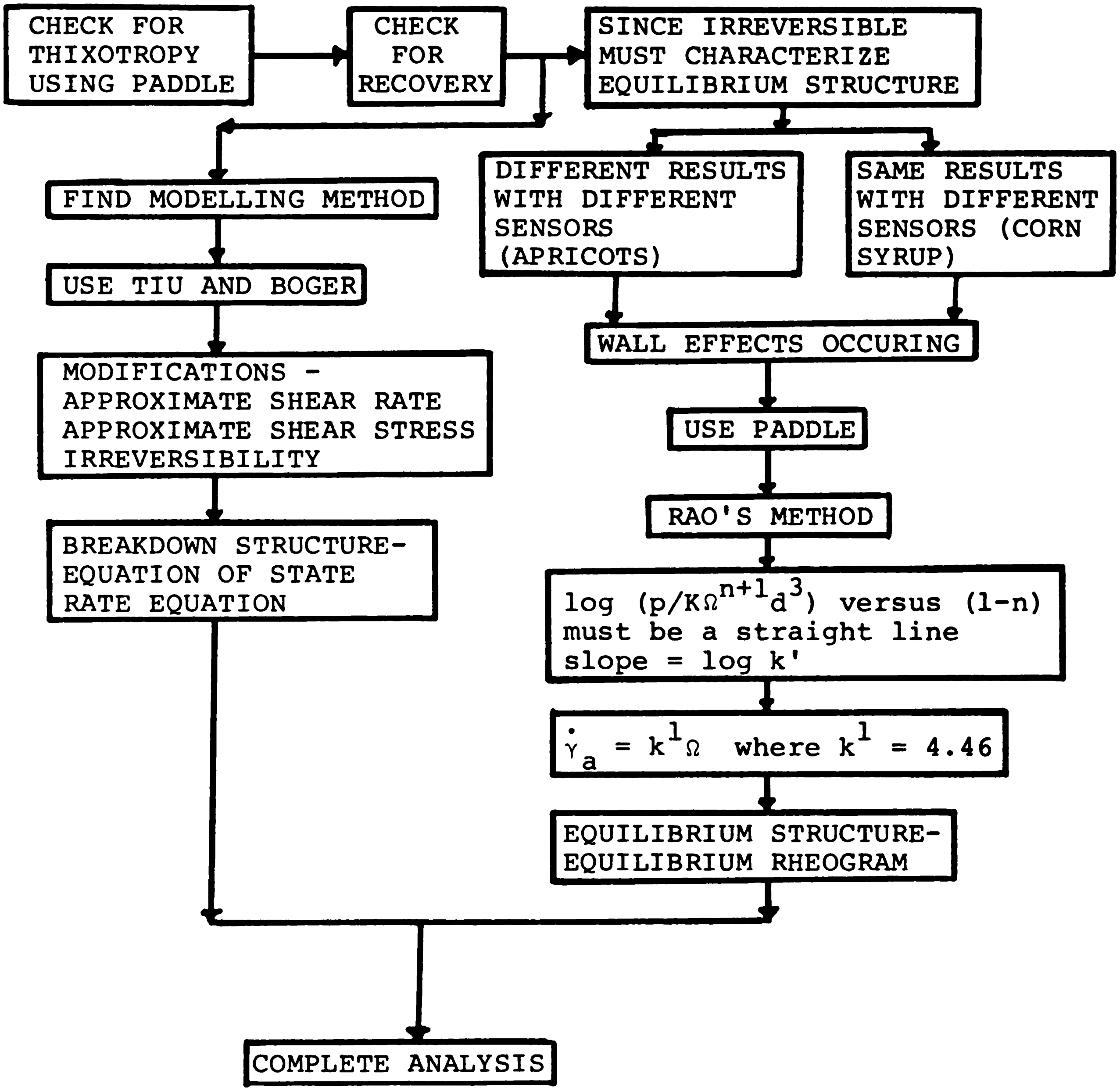
CHECK FOR THIXOTROPY USING PADDLE
CHECK FOR RECOVERY
SINCE IRREVERSIBLE MUST CHARACTERIZE EQUILIBRIUM STRUCTURE
FIND MODELLING METHOD
DIFFERENT RESULTS WITH DIFFERENT SENSORS (APRICOTS)
SAME RESULTS WITH DIFFERENT SENSORS (CORN SYRUP)
USE TIU AND BOGER
WALL EFFECTS OCCURING
MODIFICATIONS - APPROXIMATE SHEAR RATE APPROXIMATE SHEAR STRESS IRREVERSIBILITY
USE PADDLE
RAO'S METHOD
BREAKDOWN STRUCTURE- EQUATION OF STATE RATE EQUATION
log $(p/K\Omega^{n+1}d^3)$ versus $(1-n)$ must be a straight line slope = log k'
$\dot{\gamma}_a = k^1\Omega$ where $k^1 = 4.46$
EQUILIBRIUM STRUCTURE- EQUILIBRIUM RHEOGRAM
COMPLETE ANALYSIS

APPENDIX C

OUTLINE OF DATA COLLECTION

Appendix C. Outline of Data Collection

1. Turn on equipment
2. Allow to equilibrate to 25°C
3. Pour sample into cup
4. Attach paddle mixer to viscometer
5. Load cup into viscometer
6. Allow to equilibrate to 25°C (5 minutes)
7. Run viscometer at constant shear rate for 10 minutes and collect torque readings
8. Have computer print out torque versus time plot
9. Rest sample for 10 or 60 minutes
10. Repeat constant shear rate test and plot
11. Collect torque readings using the angular velocity range, 10-120 rpm
12. Have computer determine n from the torque versus angular velocity curve
13. Have computer calculate K using Rao's method (1975)
14. Repeat steps 3-13 for each sample used